CHAPTER 6
NUMERICAL RESULTS

In this section, the results of this study are described in detail. The results of linear, non-linear and 2D models associated with pulp washing are obtained using the technique of QHCM. The comparisons are presented with previously published results to prove the efficiency and superiority of the present numerical scheme. Further, the convergence, stability, and efficiency of the method are checked and compared with the previous techniques.

6.1 NUMERICAL RESULTS OF LINEAR MODEL-1

The linear model -1 discussed in the last chapter is solved with the help of the proposed method, i.e., QHCM. The breakthrough curve is used to express the numerical results for the concentration of solute at the exit level. The present results are compared with the numerical results of Grähs (1974). Mittal et al. (2013) also derived the numerical solution of this model using CHCM and proved the superiority of the method over previous techniques.

6.1.1 Comparison of Analytic and Numerical Results

The linear model is solved using the present technique. The results for exit solute concentration with respect to time is obtained for Pe=1,10 and 40 by dividing the domain into 30 elements. The comparison of numerical results derived by applying QHCM with the results of Grähs (1974) is presented in Figure 6.1. It is further noticed from the figure that the numerical results derived using QHCM are in best match with analytic results. Also, the exit solute concentration is decreasing with an increase in time. Also, with the increase in time, the solution profiles for different values of *Pe* are converging to steady-state conditions which validates the convergence criteria.

6.1.2 Comparison with Literature Data

In this study, the numerical results achieved using QHCM are compared with numerical results using the CHCM derived by Mittal et al. (2013) for *Pe* = 1, 10, and 40. The solution profiles are obtained by dividing the whole domain into 30 elements. The comparison of QHCM and previously used technique CHCM is presented in Table 6.1. It is observed that the numerical value of the concentration of solute at the exit level

obtained with QHCM is decreasing more rapidly with time in comparison to CHCM. Moreover, the results derived using the present technique are in good agreement with the analytic solution. The numerical results are better than the earlier technique, i.e., CHCM, even for the large value of the parameter, the efficiency of the method is obtained because the solution profiles are smoothly converging to zero. The results of absolute error are compared between QHCM and CHCM for 20, 30, and 40 elements. The results are calculated for *Pe*=40 and are depicted in Figure 6.2. It is further noticed that the absolute error using QHCM is less in comparison with CHCM. Also, Figure 6.2 portrayed that the numerical results show the least absolute error with the division of domain into more elements.

Table 6.1 Comparison of exit solute concentration with respect to exact and numerical solutions

	Pe = 1			Pe = 10			Pe = 40		
Time	Analytic	QHCM	CHCM (Mittal et al., 2013)	Analytic	QHCM	CHCM (Mittal et al., 2013)	Analytic	QHCM	CHCM (Mittal et al., 2013)
0	1.000E+0	1.000E+0	1.000E+0	1.000E+0	1.000E+0	1.000E+0	1.000E+0	1.000E+0	1.000E+0
0.3	3.326E-01	3.324E-01	3.315E-01	9.629E-01	9.620E-01	9.614E-01	1.000E+0	1.000E+0	9.620E-01
0.6	1.612E-01	1.610E-01	1.597E-01	7.778E-01	7.761E-01	7.790E-01	9.828E-01	9.817E-01	7.768E-01
0.9	3.784E-02	3.801E-02	3.799E-02	3.225E-01	3.202E-01	3.194E-01	4.108E-01	4.028E-01	3.219E-01
1.2	1.833E-02	1.834E-02	1.807E-02	1.854E-01	1.851E-01	1.838E-01	1.463E-01	1.425E-01	1.850E-01
1.5	4.304E-03	4.250E-03	4.583E-03	5.605E-02	5.596E-02	5.643E-02	8.823E-03	8.486E-03	5.595E-02
1.8	2.085E-03	2.073E-03	2.376E-03	3.013E-02	3.009E-02	3.076E-02	1.727E-03	1.661E-03	3.009E-02
2.1	4.895E-04	4.874E-04	7.283E-04	8.535E-03	8.526E-03	9.105E-03	5.119E-05	4.88E8-05	8.527E-03
2.4	2.372E-04	2.328E-04	4.015E-04	4.518E-03	4.276E-03	4.895E-03	8.095E-06	7.627E-06	4.516E-03
2.7	5.567E-05	5.527E-05	8.902E-05	1.259E-03	1.175E-03	1.394E-03	1.818E-07	1.850E-07	1.266E-03
3	2.697E-05	2.654E-05	3.843E-05	6.629E-04	6.098E-04	7.345E-04	2.623E-08	4.157E-08	6.646E-04
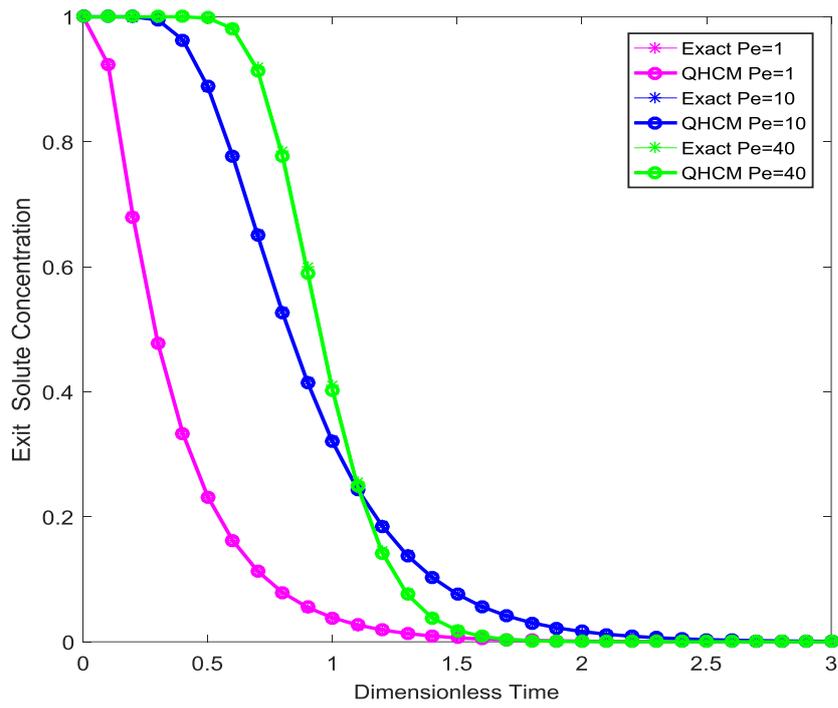
Figure 6.1 Comparison of the exact solution and QHCM for 30 elements.
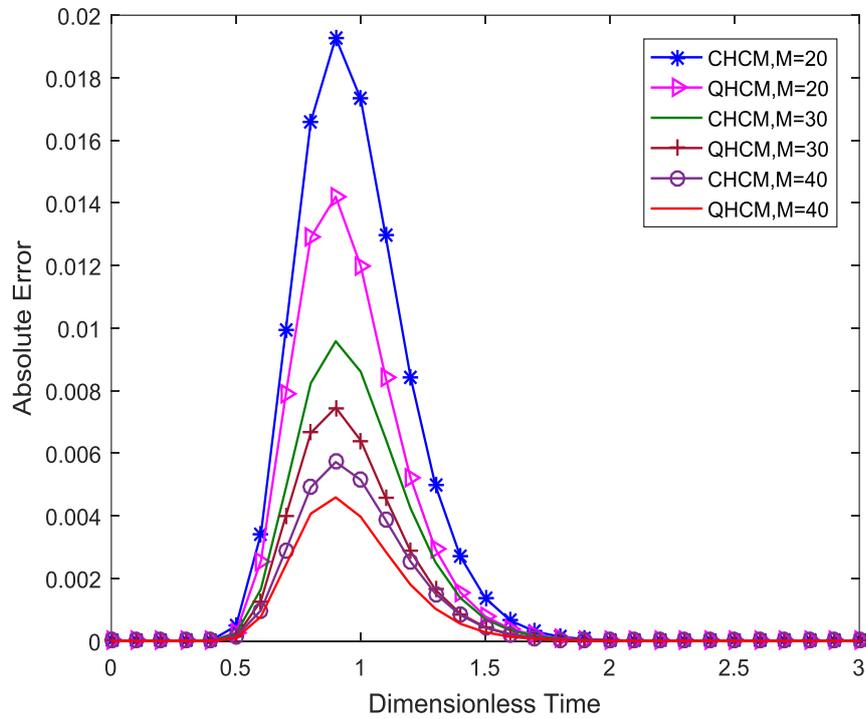
Figure 6.2 Comparison of absolute error between QHCM and CHCM for *Pe*=40

6.1.3 Influence of Number of Elements

The results for exit solute concentration by partitioning the domain into different elements help to check the computational cost of a numerical technique. The results for the concentration of solute for this model are obtained by dividing the domain into 10,40,80 and120 elements. The effect of the division of the domain into different partitions on the solution profile is shown in Figure 6.3. The error ascertained by this method is minimal in the case of the number of elements N=40 and N=80. However, in the case for N=10, the results vary when compared with analytic ones. So, it can be observed that when the partitions are increased, the number of equations increases but the accuracy of the results compensates for it. Whereas, when the number of elements is increased to 120, the solution profile does not behave properly.

6.1.4 Error Analysis

The relative error helps to check the accuracy of the results. The formula for relative error is discussed in chapter 3. In the present study, the solution is obtained using QHCM, and a comparison with the analytic solution is made in terms of relative error. The results of relative error using QHCM and CHCM are graphically shown in Figures 6.4 to 6.6. The decrease in relative error is observed when the number of elements is increased. It can be seen from Figure 6.4 that for Pe=1, the relative error in the case of CHCM with 10 elements fluctuates with a maximum magnitude of 1.4×10^{-1} (approximately). However, in QHCM relative error is almost zero. Also, it can be seen from Figure 6.5 that for Pe=10, the magnitude of the relative error using QHCM is nearer to zero as compared with CHCM for when the domain is partitioned into 40 elements. The relative error for QHCM, therefore, matches best with the analytic solution. However, when CHCM is applied, the magnitude of relative error goes down to 2.6×10^{-4} (approximately), which is comparatively less than for the value of Pe=1 and 10. The relative error for both the methods is the same for the time up to 2 seconds but from 2 to 3 seconds, it starts decreasing in the case of CHCM. However, in QHCM relative error is almost zero and the results are found to be more stable and convergent in the case of QHCM as compared to CHCM.
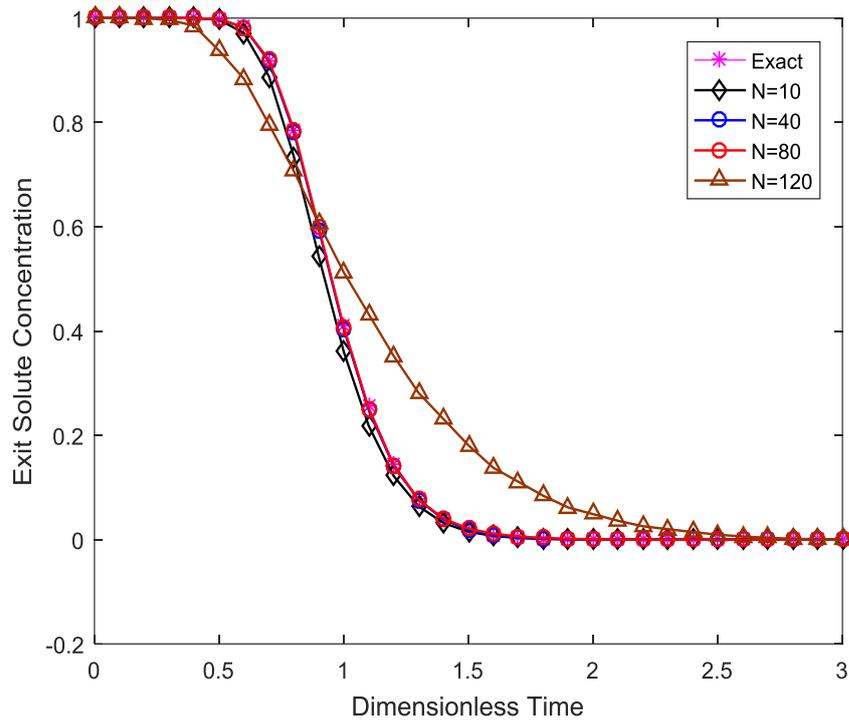
Figure 6.3 Comparison of exit solute concentration for *Pe*=40 by dividing the domain into the various number of elements.
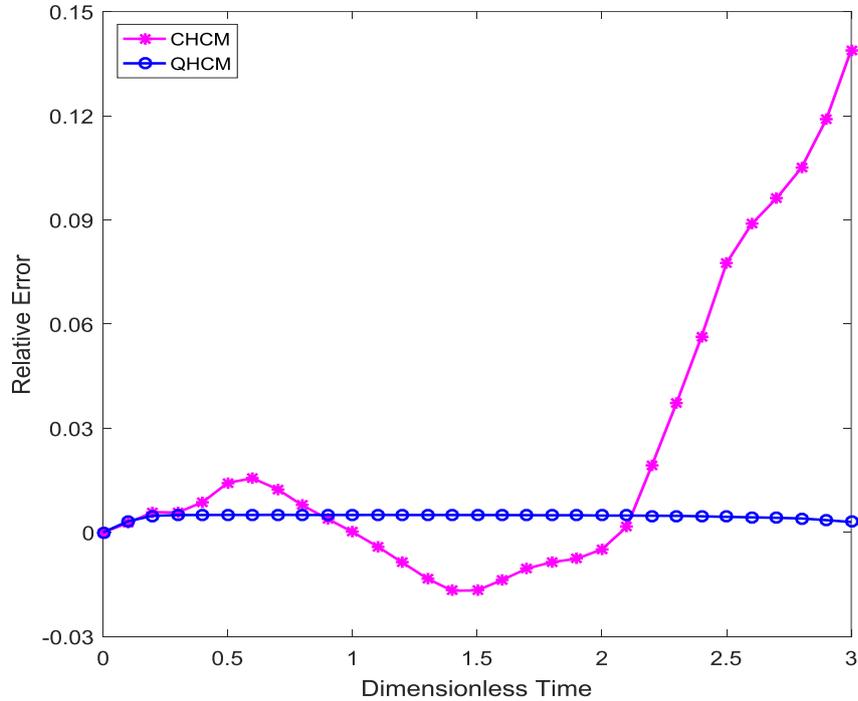
Figure 6.4 Relative error comparison between QHCM and CHCM for *Pe*=1, M=10
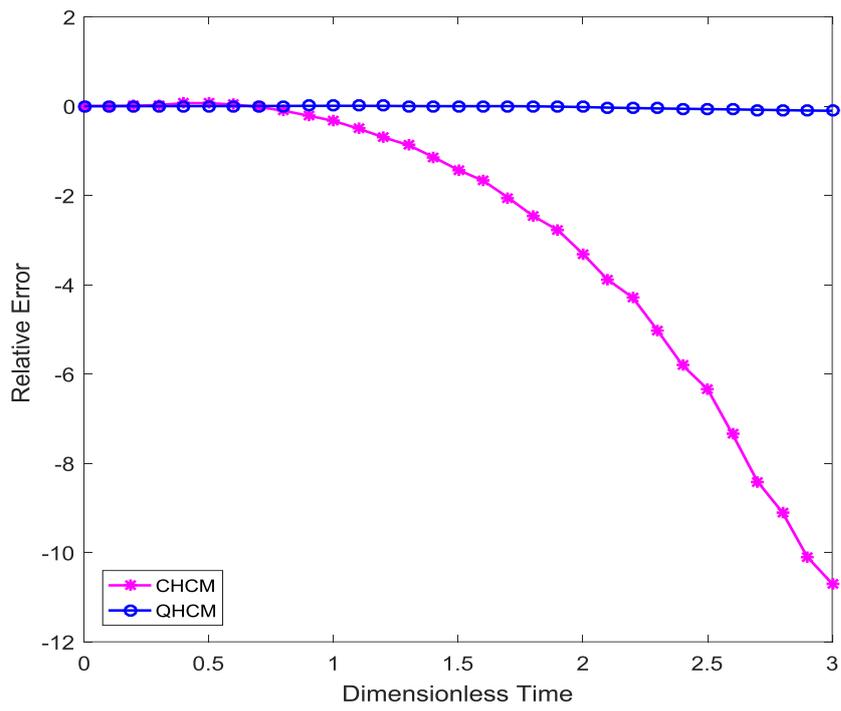
Figure 6.5 Relative error comparison between QHCM and CHCM for *Pe*=10, M=40
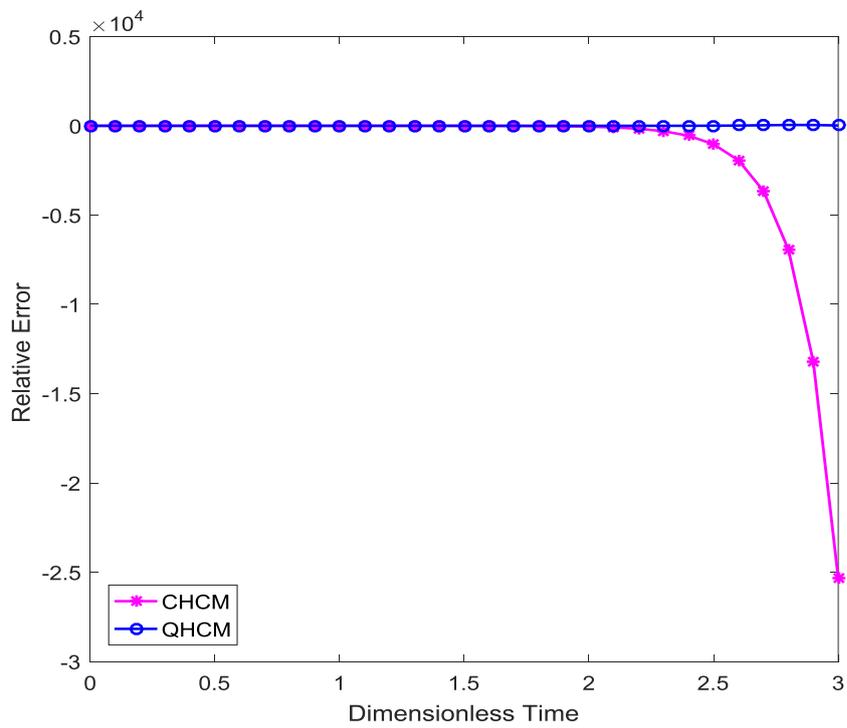
Figure 6.6 Relative error comparison between QHCM and CHCM for *Pe*=40 and M=40

6.1.5 Stability Analysis Using Norms and Comparison with CHCM

The stability analysis for the QHCM is checked by using the supremum norms ($\|L\|_\infty$) and Euclidean norm ($\|L\|_2$) for the linear model. The maximum absolute error using QHCM and CHCM is compared with the solution given by Grähs (1974). In Table 6.2, the comparison of maximum norms ($\|L\|_\infty$) for both techniques is presented. It can be observed that the maximum absolute error using QHCM is least as compared with CHCM in all the cases. Even for the large value of Pe, a small amount of error is seen in the case of QHCM. Table 6.3 shows the comparison of the Euclidean norm for different values of Pe between the two methods. A major difference is observed between the two methods. It can be observed that the value of the Euclidean norm using QHCM is least as compared with CHCM in all the cases. Moreover, when the partitions are increased, a decrease in the Euclidean norm is observed. Also, both norms lie between 0 and 1. Keeping the above aspects in view, it can be concluded that the QHCM is a better technique to solve the BVPs.

6.2 NUMERICAL RESULTS OF LINEAR MODEL-2

The linear model -2 discussed is solved with the help of the proposed method. The numerical results derived for the concentration of solute at the exit level are expressed with the breakthrough curve. Brenner (1962) derived the exact solution of the model using the method of Laplace Transform. This model is also solved numerically by Arora et al. (2006) using OCFE and by Ganaie et al. (2013) using CHCM.

6.2.1 Comparison Between Analytic and Numerical Results

The QHCM is used to solve the problem and the comparison is made between numerical results and the exact solution. The comparison of results is shown in Table 6.4. It is also noticed from the table that the concentration profile converges to zero quickly when there is an increase in time. A good agreement is seen between the numerical results and the exact solution.

Table 6.2. Comparison of $\|L\|_\infty$ norm CHCM and QHCM

Number of elements	Pe = 1		Pe = 10		Pe = 40	
	CHCM	QHCM	CHCM	QHCM	CHCM	QHCM
M=10	3.991E-03	3.262E-03	4.876E-02	1.493E-03	2.801E-01	5.751E-02
M=20	3.503E-03	8.101E-04	5.180E-03	4.100E-03	2.709E-01	1.923E-02
M=30	2.562E-03	7.303E-04	3.040E-03	2.830E-03	2.690E-01	9.583E-03
M=40	2.514E-03	5.804E-04	2.640E-03	2.200E-03	2.682E-01	7.552E-03

Table 6.3. Comparison of $\|L\|_2$ norm CHCM and QHCM

Number of elements	Pe = 1		Pe = 10		Pe = 40	
	CHCM	QHCM	CHCM	QHCM	CHCM	QHCM
M=10	2.412E-03	1.752E-03	9.025E-02	1.091E-02	1.663E-01	3.453E-02
M=20	1.383E-03	3.091E-04	2.430E-03	2.120E-03	1.149E-01	8.165E-03
M=30	8.091E-04	2.704E-04	1.133E-03	1.083E-03	9.236E-02	3.318E-03
M=40	6.722E-04	2.856E-04	8.872E-04	7.117E-04	7.974E-02	2.175E-03

6.2.2 Comparison with Previous Results

The comparisons are made between the numerical results for concentration profiles at the exit level using the algorithm of QHCM with the numerical results obtained by Arora et al. (2006) using the technique OCFE and with the technique CHCM which is used by Ganaie et al. (2013). The relative error for derived numerical results of exit solute concentration is compared with the analytic solution for Pe=80 given by Brenner (1962). The relative error is calculated results of Arora et al. (2006) (OCFE) and Ganaie et al. (2013) (CHCM) with analytic values of Brenner (1962). These errors are presented graphically in Figure 6.7. It is noted from the figure that the relative error with QHCM is negligible as compared to OCFE and CHCM.

Table 6.4 Comparison between the exact solution and numerical results derived using QHCM

Time	Pe = 1		Pe = 40		Pe = 80	
	Brenner (1962)	**QHCM**	**Brenner (1962)**	**QHCM**	**Brenner (1962)**	**QHCM**
0.0	1.0000E+00	1.0000E+00	1.0000E+00	1.0000E+00	1.0000E+00	1.0000E+00
0.2	9.9510E-01	9.9383E-01	1.0000E+00	1.0000E+00	1.0000E+00	1.0000E+00
0.4	8.9851E-01	8.9351E-01	1.0000E+00	1.0000E+00	1.0000E+00	1.0000E+00
0.6	7.1771E-01	7.1330E-01	1.0000E+00	1.0000E+00	1.0000E+00	1.0000E+00
0.8	5.3788E-01	5.3234E-01	9.7461E-01	9.7574E-01	9.9749E-01	9.9748E-01
1.0	3.9090E-01	3.8611E-01	4.7780E-01	4.7836E-01	4.8431E-01	4.8855E-01
1.2	2.8012E-01	2.7808E-01	4.4936E-02	4.5409E-02	9.2825E-03	9.3303E-03
1.4	1.9925E-01	1.9890E-01	9.9034E-04	9.9231E-04	7.6158E-06	7.6242E-06
1.6	1.4127E-01	1.4441E-01	7.9001E-06	7.9104E-06	7.1183E-10	7.0080E-10
1.8	9.9870E-02	9.9853E-02	3.1110E-08	3.0927E-08	1.5032E-14	1.4942E-14
2.0	7.0581E-02	7.0490E-02	7.4063E-11	7.3890E-11	-7.7170E-20	-1.4250E-17
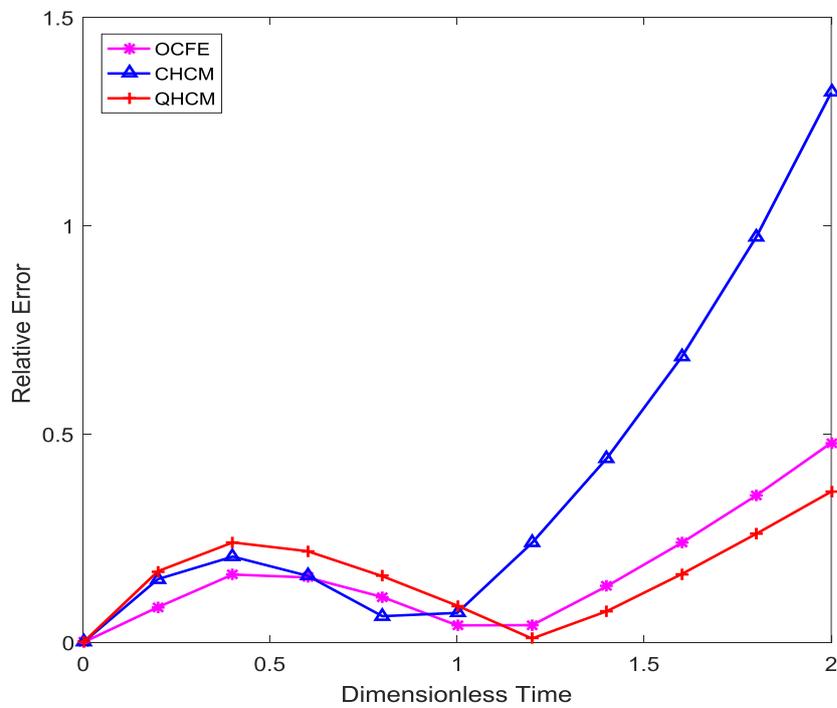
Figure 6.7 Relative error comparison of QHCM with OCFE and CHCM for *Pe*=80.

6.2.3 Effect of Number of Elements

The selection of step size or division of domain plays important role in measuring accuracy. Arora et al. (2005) explained that the choice of large step size in the domain of space and time helps to maintain the best agreement for the numerical solution and analytical solution with minimum error. The model is solved for different partitions using the present method for *Pe*=40 and the results are presented in terms of relative error for a wider range division of domain in Figure 6.8. The relative error is calculated for the division of the domain into 20,40 and 80 elements. The relative error is approaching to zero as the domain is partitioned into more elements. Also, both numerical and analytic solutions are matching for the division of the domain into 80 elements.
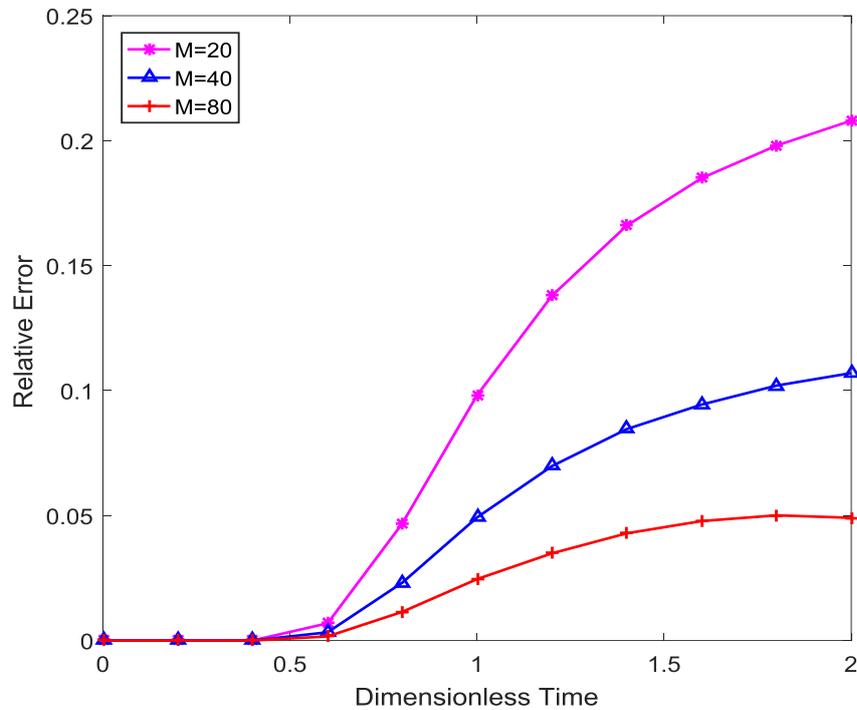
Figure 6.8 Comparison of relative error by division of domain into different elements for *Pe*=40.

6.2.4 Stability Analysis and CPU Time

The relative error, norms, and CPU time play a very important role to check the efficiency of the method (Jannesari and Tatari, 2020). The reported CPU time is the total elapsed time of the entire process. The model equation is solved for *Pe*=1, 10, and 40 by dividing the domain into different elements. The numerical results of supremum

norms ($\|L\|_\infty$) and Euclidean norms ($\|L\|_2$) for different partitions are computed and reported in Table 6.5. It is noticed from the table that both the norms lie within 0 and 1 and this proves the stability of the method. Further, it can be discovered that both norms are decreasing when the domain is partitioned into more elements. The CPU time in solving the model is very less with a minimum time of 1.5 seconds and a maximum time is 3.92 seconds. Hence, the method with better accuracy is giving better accuracy with less CPU time.

Also, the maximum absolute error derived using the exact solution given by Brenner (1962) for QHCM and CHCM is compared. It has been observed that for this model, the absolute error obtained using QHCM is less as compared to CHCM in all the cases given in Table 6.6. Further, a small amount of absolute error is seen in the case of QHCM, even for the large value of parameter *Pe*. Therefore, it can be concluded that numerical result obtained using QHCM agrees well with an analytic solution in comparison to CHCM.

The values of the Euclidean norm using the analytic solution given by Brenner (1962) are calculated for CHCM and QHCM. The comparison of this norm between both techniques is presented in Table 6.7. It is observed that the results obtained using QHCM are either at par or below the error noticed by the CHCM. Hence, the stability conditions given by Arora et al. (2005) are satisfied for QHCM and better accuracy is achieved by using QHCM in comparison with CHCM.

Table 6.5 Results for supremum norms ($\|L\|_\infty$), Euclidean norms ($\|L\|_2$) and CPU time

M	$\|L\|_2$			$\|L\|_\infty$			CPU time (in sec)		
	Pe=1	Pe=10	P=40	Pe=1	Pe=10	Pe=40	Pe=1	Pe=10	Pe=40
10	3.832E-3	1.378E-3	5.120E-4	1.383E-2	1.461E-2	2.202E-2	1.72	1.47	1.51
20	3.741E-3	1.093E-3	4.892E-4	8.671E-3	9.323E-3	3.261E-3	2.51	2.32	2.14
30	3.674E-3	1.011E-3	4.757E-4	6.812E-3	7.380E-3	2.014E-3	2.93	2.81	2.81
40	3.380E-3	1.003E-3	4.102E-4	5.506E-3	6.731E-3	1.100E-3	3.90	3.73	3.80

Table 6.6 Comparison of maximum absolute error for CHCM and QHCM

M	Pe=1		Pe=10		Pe=40	
	CHCM	QHCM	CHCM	QHCM	CHCM	QHCM
10	1.951E-01	1.383E-02	2.440E-01	1.461E-02	2.441E-01	2.202E-02
20	1.745E-01	8.671E-03	2.193E-01	9.323E-03	2.100E-01	3.261E-03
30	1.672E-01	6.812E-03	2.101E-01	7.380E-03	1.985E-01	2.014E-03
40	1.646E-01	5.506E-03	2.053E-01	6.731E-03	1.912E-01	1.100E-03

Table 6.7 Comparison of $\|L\|_2$ (Euclidean) norm for CHCM and QHCM

M	Pe=1		Pe=10		Pe=40	
	CHCM	QHCM	CHCM	QHCM	CHCM	QHCM
10	1.381E-01	3.832E-03	1.53E-01	1.378E-03	1.201E-01	5.120E-04
20	8.674E-02	3.741E-03	9.93E-02	1.093E-03	7.674E-02	4.892E-04
30	6.812E-02	3.674E-03	7.88E-02	1.011E-03	6.041E-02	4.757E-04
40	5.781E-02	3.380E-03	6.73E-02	1.003E-03	5.150E-02	4.102E-04

6.3 VERIFICATION OF LINEAR MODEL-3

The model is solved using the present method of QHCM. Zheng and Gu (1996) presented a detailed explanation of this model with the exact solution. Arora et al (2006) have compared the relative error of OCM and OCFE for this model and noticed improved results. Gupta and Kukreja (2012), Ganaie et al. (2013), and Robalo et al. (2013) also solved this model with CSCM, CHCM, and MFEM respectively.

6.3.1 Comparison of Numerical and Analytic Results

The results obtained using the QHCM for different parameters are summarized in Table 6.8 and the values are in conformity with the analytic solution obtained by Zheng and Gu (1996). The numerical results are derived by dividing the domain into 25 and 50 number of elements for different ranges of parameters such as Pe, Bi, and μ. The best match of numerical and analytic results is noticed in the table when more elements are added in the partitions. It is also observed that the difference between numerical and analytic results decreases when the number of elements in the domain increases.

6.3.2 Comparison of the Number of Elements

The results obtained using the QHCM are compared with the previously published result of Ganaie et al. (2013) using CHCM. The numerical results compared for Pe=10, Bi=1.5, μ=0.0142 and Pe=20, Bi=5, μ=0.033 and summarized it in Table 6.9. The exact solution obtained by Zheng and Gu (1996) is considered for comparison. Ganaie et al. (2013) partitioned the domain into 200 elements, but, in this work, the results match exacts ones only with 50 number of elements. This proves that the present results are better with a smaller number of equations. So, the computational cost is reduced with the present technique.

6.3.3 Comparison with Literature Data in Terms of Relative Error

A comparison between the QHCM, CSCM (Gupta and Kukreja, 2012), MFEM (Robalo et al., 2013), and CHCM (Ganaie et al., 2013) is made for different parameters by taking the same number of partitions of the domain. The results are derived for parameters Pe=20, Bi=5, μ=0.033. The results of relative error from these methods and present technique are compared in Figure 6.9. Also, the results of relative error for Pe=10, Bi=1.5, and μ=0.0142 are shown in Figure 6.10. It is noticed that relative error is least in the case of QHCM as compared to other methods in both cases as shown in these figures.

6.3.4 Stability analysis using QHCM and CPU Time

The stability of the present method is checked by comparing the results for supremum norms ($\|L\|_\infty$) and Euclidean norms ($\|L\|_2$) with previously published results. Both norms are calculated by using the numerical values for exit solute concentration of published results with CHCM, CSCM, and MFEM. The norms are calculated for Pe=10, Bi=1.5, μ=0.0142, and Pe=20, Bi=5, μ=0.033, and the results are presented in Table 6.10. It is evident from the table that values calculated for both the norms $\|L\|_2$ and $\|L\|_\infty$ using QHCM are having least value than previously published methods and hence the method is found to be more stable. The table also reflects those values of both $\|L\|_2$ and $\|L\|_\infty$ norms using QHCM are decreasing when the number of elements is increased.

The time consumed to solve the model is also an important factor to implement the method for numerical solutions. The CPU time to complete the process is also noted while performing the processor and compared with the published results of Gupta and Kukreja (2012) in Table 6.11. It is observed from the table that the CPU time consumed using the QHCM is 1.9730 seconds when the domain is divided into 25 elements, while Gupta and Kukreja (2012) reported that it takes 6.6746 seconds using the CSCM. Also, Gupta and Kukreja (2012) have shown in their study that CSCM takes less time than OCM and OCFE. However, the present study reflects the fact that QHCM takes very little time as compared to the previous methods.

6.3.5 Effect of Pe and Bi on the Concentration Profile

The *Pe* helps to estimate the results with more accuracy (Jia et al., 2013). Also, Szukiewicz (2001) observed that the accuracy of calculations is higher influenced by *Bi*. The comparison of the solution profile for different values of the *Bi*, *Pe*, and *μ* is derived using the present method and presented in Figure 6.11. It is observed that when *Pe* is greater than 20 and *Bi* is greater than 5, the adsorbed solute takes a larger time to strain out from the surface of the fiber. It is for this reason that small *Pe* creates more back mixing and small *Bi* reduces the equilibrium constant. In a study, Arora et al. (2006) and Ganaie et al. (2013) also concluded that $Pe < 20$ and $Bi < 5$ are of practical importance.

Table 6.8 Comparison of numerical results with exact for different Pe and Bi

Time	QHCM Pe=10, Bi=1.5, μ =0.0142			QHCM Pe=20, Bi=5, μ =0.033			QHCM Pe=60, Bi=7.5, μ =0.033		
	Exact	N =25	N =50	Exact	N =25	N =50	Exact	N =25	N=50
0	1.000E+0	1.000E+0	1.000E+0	1.000E+0	1.000E+0	1.000E+0	1.000E+0	1.000E+0	1.000E+0
0.2	9.998E-01	9.994E-01	9.998E-01	9.983E-01	9.980E-01	9.983E-01	9.991E-01	9.990E-01	9.991E-01
0.4	9.620E-01	9.614E-01	9.620E-01	9.938E-01	9.941E-01	9.938E-01	9.983E-01	9.979E-01	9.983E-01
0.6	7.768E-01	7.747E-01	7.768E-01	9.083E-01	9.059E-01	9.083E-01	9.937E-01	9.928E-01	9.935E-01
0.8	5.272E-01	5.253E-01	5.272E-01	6.533E-01	6.488E-01	6.533E-01	8.508E-01	8.460E-01	8.506E-01
1	3.218E-01	3.201E-01	3.218E-01	3.709E-01	3.665E-01	3.709E-01	4.254E-01	4.201E-01	4.253E-01
1.2	1.849E-01	1.848E-01	1.849E-01	1.784E-01	1.767E-01	1.784E-01	1.160E-01	1.149E-01	1.160E-01
1.4	1.026E-01	1.021E-01	1.026E-01	7.695E-02	7.569E-02	7.698E-02	2.004E-02	1.959E-02	2.003E-02
1.6	5.585E-02	5.558E-02	5.585E-02	3.090E-02	3.038E-02	3.090E-02	2.520E-03	2.458E-03	2.520E-03
1.8	3.001E-02	2.989E-02	3.001E-02	1.182E-02	1.167E-02	1.182E-02	2.540E-04	2.477E-04	2.540E-04
2	1.600E-02	1.598E-02	1.601E-02	4.379E-03	4.308E-03	4.379E-03	2.179E-05	2.156E-05	2.179E-05

Table 6.9 Comparison of numerical results of QHCM with CHCM

Time	Pe=10, Bi=1.5, μ=0.0142			Pe=20, Bi=5, μ=0.033		
	Exact	N=200 (CHCM)	N=50 QHCM	Exact	N=200 (CHCM)	N=50 (QHCM)
0	1.000E+00	1.000E+00	1.000E+00	1.000E+00	1.000E+00	1.000E+00
0.2	9.998E-01	9.994E-01	9.998E-01	9.983E-01	9.983E-01	9.983E-01
0.4	9.620E-01	9.620E-01	9.620E-01	9.938E-01	9.938E-01	9.938E-01
0.6	7.768E-01	7.768E-01	7.768E-01	9.083E-01	9.083E-01	9.083E-01
0.8	5.272E-01	5.272E-01	5.272E-01	6.533E-01	6.533E-01	6.533E-01
1	3.218E-01	3.218E-01	3.218E-01	3.709E-01	3.709E-01	3.709E-01
1.2	1.849E-01	1.849E-01	1.849E-01	1.784E-01	1.784E-01	1.784E-01
1.4	1.026E-01	1.026E-01	1.026E-01	7.695E-02	7.692E-02	7.798E-02
1.6	5.585E-02	5.585E-02	5.585E-02	3.090E-02	3.090E-02	3.090E-02
1.8	3.001E-02	3.001E-02	3.001E-02	1.182E-02	1.182E-02	1.182E-02
2	1.600E-02	1.600E-02	1.600E-02	4.379E-03	4.378E-03	4.379E-03

Table 6.10 Comparison of results of $\|L\|_2$ and $\|L\|_\infty$ norms

	Pe=10, Bi=1.5, μ=0.0142				Pe=20, Bi=5, μ=0.033			
	QHCM	MFEM	CSCM	CHCM	QHCM	MFEM	CSCM	CHCM
$\|L\|_2$	3.626E-6	6.026E-6	5.8515E-6	1.771E-5	3.441E-6	5.483E-6	2.281E-6	4.881E-5
$\|L\|_\infty$	9.900E-6	2.580E-5	1.000E-5	6.000E-5	1.000E-5	2.000E-5	1.000E-5	2.100E-4

Table 6.11 Comparison in total elapsed time (in sec) between QHCM and CSCM for Pe=60, Bi=7.5, and μ=0.033

Number of elements (N)	QHCM	CSCM
25	1.9730	6.6746
50	2.8427	7.6188
100	5.2921	9.7043
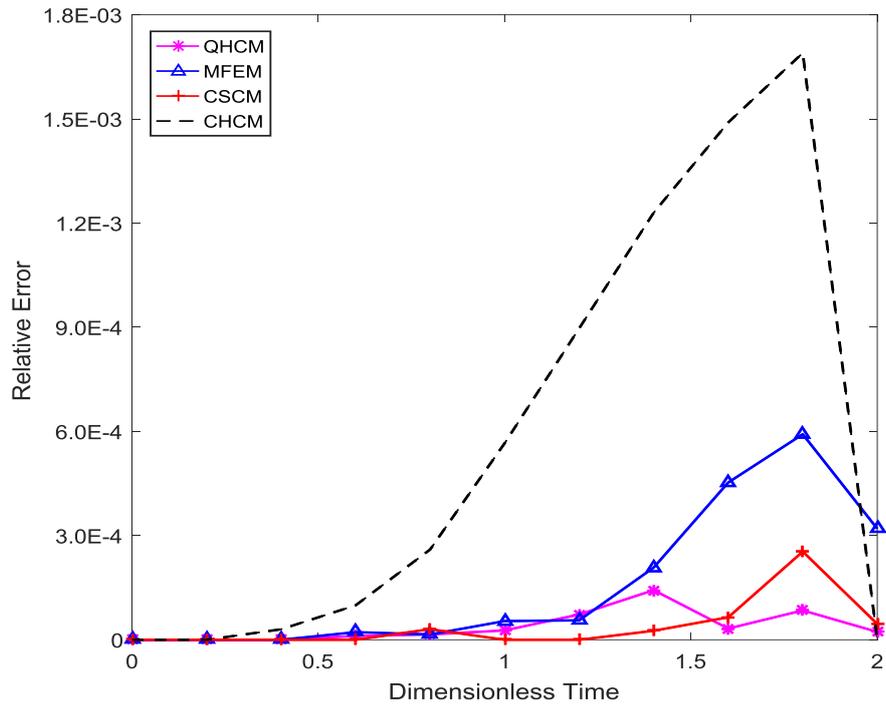
Figure 6.9 Relative Error comparison for Pe=20, Bi=5, μ=0.033
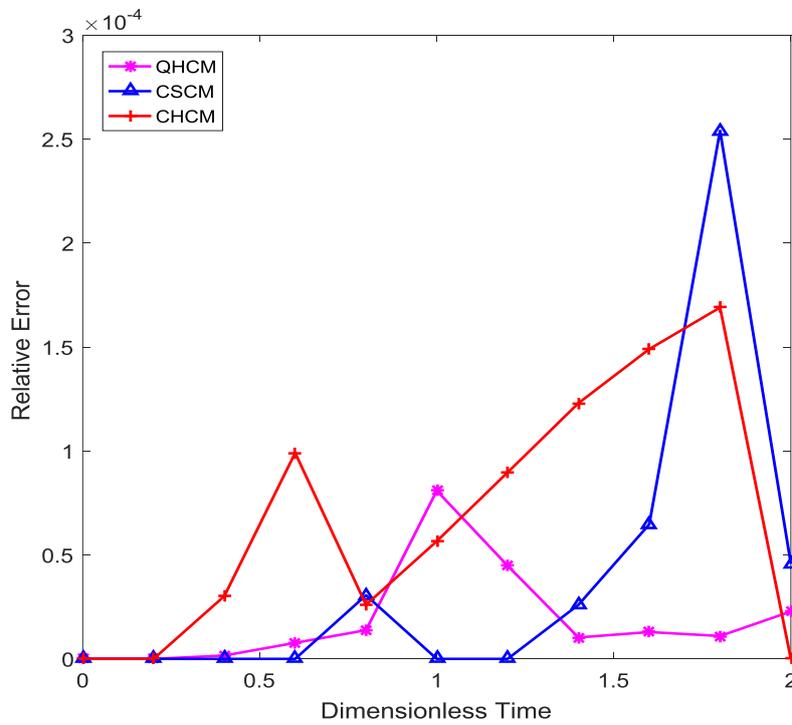
Figure 6.10 Comparison of CSCM, CHCM and QHCM for Pe=10, Bi=1.5, μ=0.0142

6.4 VERIFICATION OF LINEAR MODEL-4

The results for exit solute concentration are obtained for different values R_d (retardation coefficient) which is defined as the removal rate of adsorbed solutes on the particle surface. Liao and Shiau (2000) derived the analytic solution for this problem. Arora et al. (2006) solved this model using OCFE and presented the relative error of the numerical solution for different values of Pe and R_d.

6.4.1 Effect of Retardation Coefficient (R_d)

Figure 6.12 displays the comparison of solution profiles for different values R_d with Pe=40. The figure indicates that for the constant value of Pe, the breakthrough curve moves slowly to a steady state condition and a large breakthrough time is needed for an increased value of R_d. It is observed that better washing can be achieved with an increase R_d from 0.85. Arora et al. (2006) explained that better washing R_d must be greater than 1.

6.4.2 Effect of large R_d for different values of Pe

The effect of large R_d varying from 2 to 10 on solution profiles is displayed in Figure 6.13 for different ranges of Pe. The figure explains that when Pe=40 and R_d=5, the solute (black liquor) is not detached from the pulp, as the exit concentration of solute is not reducing. Figure 6.13 displays that the value of R_d=2 gives better results when the Pe is decreased. For Pe=40, the solution profile for R_d=2 moves to steady state condition while for R_d= 5, the solution profiles are not converging to steady state condition. It is observed from the figure that when R_d is increased from 2, the breakthrough curves become broadened, and the solution profiles do not reach steady state condition and take a long time to converge to steady state condition. It is noticed from the figure that as soon as the value of R_d is increased, the curve of the mass-transfer zone does not show better washing results. The constant value of R_d and
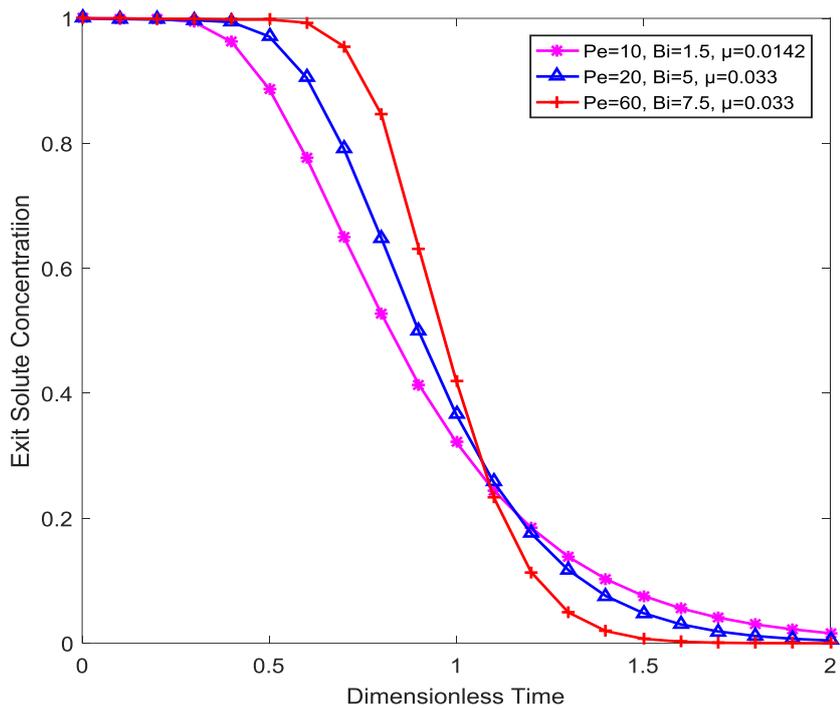
Figure 6.11 Effect of different values of *Pe* and *Bi* on the concentration of solute at exit level
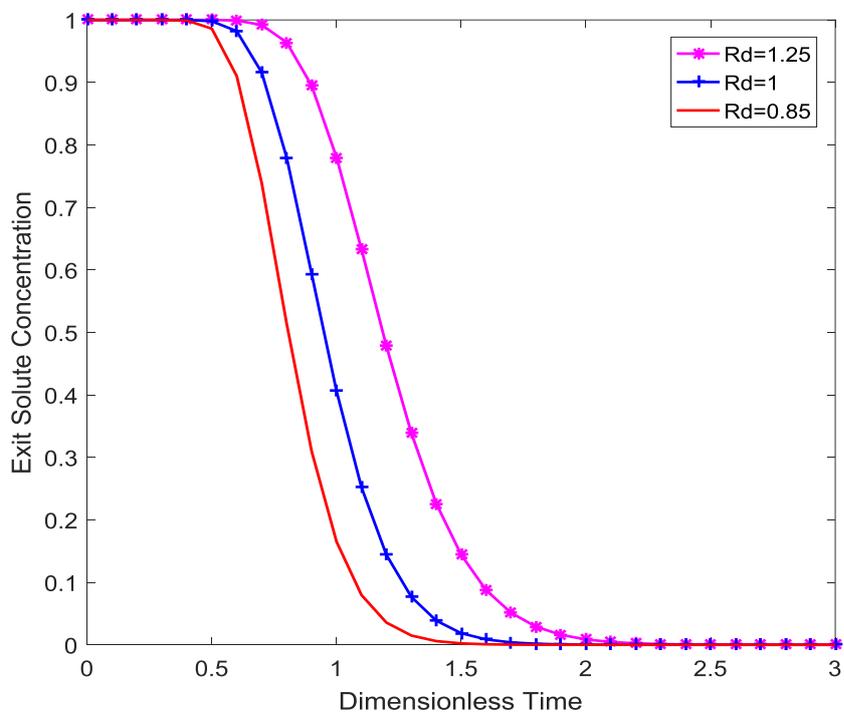
Figure 6.12 Effect on exit solute concentration for different values of R_d

decreasing value of *Pe* means the dispersion coefficient is increased in the case when the length of bed thickness and interstitial velocity both are kept unchanged. The reason is that the increase in R_d, affects the space and time gradients in comparison with the dispersion term. Moreover, when the value of R_d is increased, there is a decrease in bed porosity and the detachment rate becomes constant which helps in reducing the impurities removal rate which is adsorbed on the surface. Hence, the solution profile takes more time to reach the steady state condition.

6.4.3 Effect of *Pe* for the Constant Value of *Rd*

Figure 6.14 displays the behavior of the washing curve for different ranges of *Pe* when the value of R_d is considered constant. It is obvious from the figure that when R_d is a constant, the higher the value of *Pe* and the steeper mass transfer zone will be obtained. According to the results noticed in figure, for a large value of *Pe*, the effluent concentration of adsorbate will quickly reach the influent concentration, but it takes a large breakthrough time. In the case when R_d is constant, the small value of *Pe* provides more mixing. The present solute started to diffuse out in a short period. The curves started to give coincident results when *Pe* is increased from 40. When the value of *Pe* is larger than 100 the breakthrough curve instantly started decreasing. In this case, the washing process is not proper, and more diffusion is caused which makes the solute diffuse out in a piston-like manner. Karahan (2006) supported the simulations of advection-diffusion depending on higher values of *Pe*.
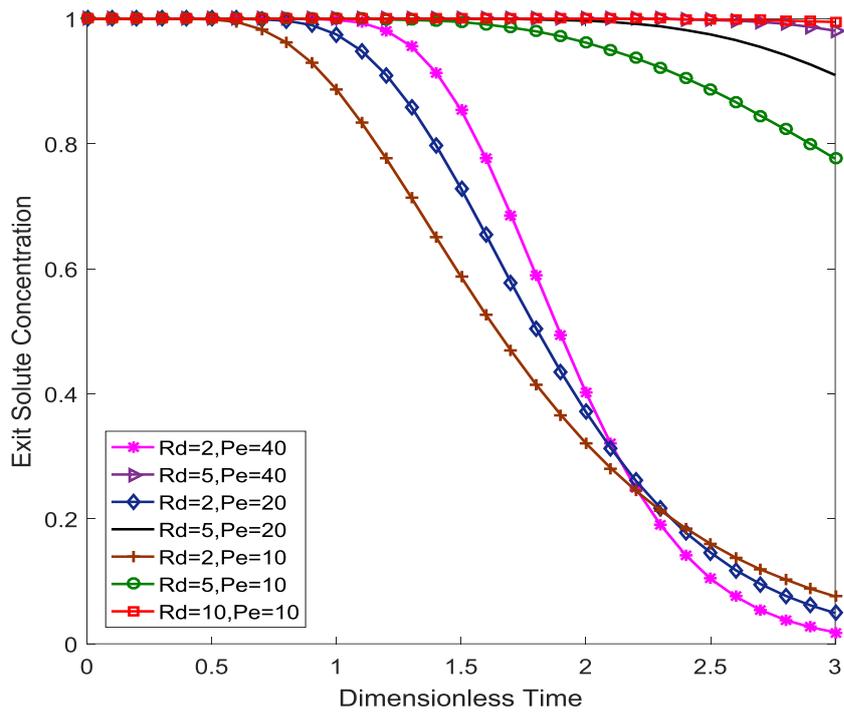
Figure 6.13 Effect on exit solute concentration for large values of R_d
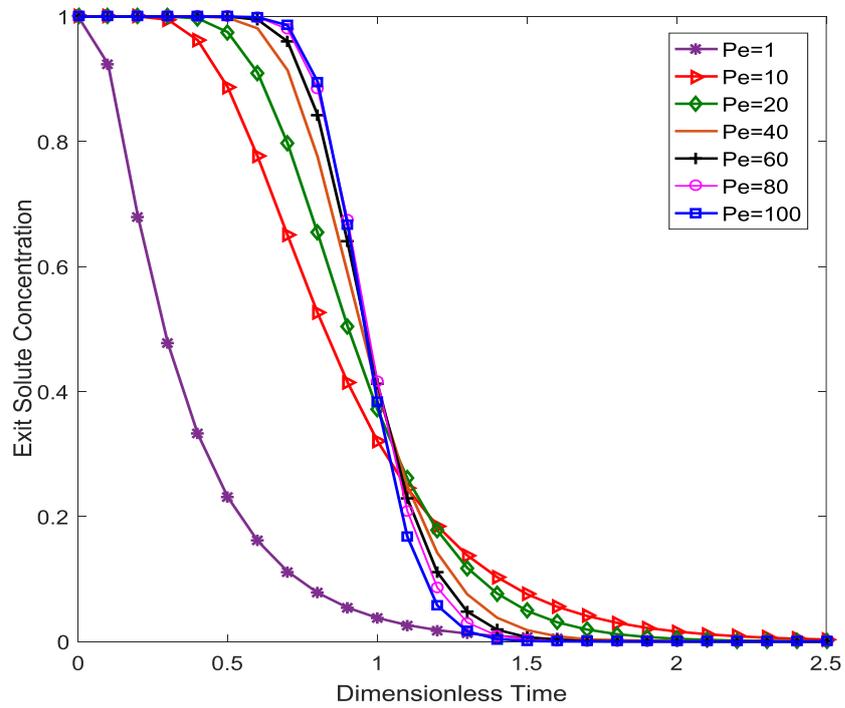
Figure 6.14 For $R_d = 1$, the effect of different values of *Pe* on the solute concentration

6.5 RESULTS OF NONLINEAR MODEL-1

The nonlinear model is solved using the QHCM for different values of parameters such as *Pe*, bed porosity, axial dispersion coefficient, and cake thickness. As the non-linear problem does not have an analytic solution, the model equations are simulated using the experimental data. The results obtained for this model are verified using the experimental data of Grähs (1974), Kukreja (1996), and Arora and Potuček (2012). This data is related to the research experiments which are performed for washing wood pulp. The applicability of the model is checked in the study using actual industrial data taken from a brown stock washer (for pulp washing) at the fourth stage of a paper mill. The detailed data of experimental values given by these authors are presented in Tables 6.12 to 6.14. Although the available experimental data varies across the paper mills, the only purpose of applying this method is to prove its efficiency in solving the model.

6.5.1 Solution Profile for Concentration at Exit Level

The non-linear model of displacement washing is solved numerically using QHCM. The mathematical model explained above is solved using the experimental data of Grähs (1974) tabulated in Table 6.15 for simulation. The method is applied by dividing the domain into the number of elements M=20,40,80. The model is solved by taking different values of *Pe*=1, 10, and 40, and the output results in terms of concentration are presented in Table 6.15. It is seen from the table that the concentration of solute at the exit level approaches zero smoothly when the number of elements (M) in the domain is increased. Besides, the solution profiles in all cases are converging to steady-state conditions with an increase in time. This proves the convergence of the method according to Onah (2002).

Table 6.12 Experimental data of washing cell of Grähs (1974)

Parameters	Values	Unit
ε	0.925-0.957	-
A_0	0.01195	m^3/kg
B_0	2.708	m^3/kg
C_0	0.225-0.655	kg/m^3
C_S	0.000	kg/m^3
C_F	63.8-106.9	kg/m^3
L	0.102-0.166	m
k_1/k_2	$4.0 \times 10^{-4} - 7.0 \times 10^{-5}$	-

Table 6.13 Washing cell experimental data of Kukreja (1996)

Parameters	Values	Unit
ε	0.954-0.986	-
A_0	0.931	m^3/kg
B_0	0.536	m^3/kg
C_0	77.3-158.95	kg/m^3
C_F	22-69.20	kg/m^3
L	0.005-0.007	m
k_1/k_2	$2 \times 10^{-4} - 7.0 \times 10^{-4}$	-

Table 6.14 Experimental data of washing cell (Arora and Potuček,2012)

Parameters	Values	Unit
ε	0.955-0.968	-
A_0	0.00052	m^3/kg
B_0	0.000052	m^3/kg
C_0	8.3341-8.3782	kg/m^3
u	$(1.9321-1.9584) \times 10^{-3}$	m/s
C_F	47.059-66.176	kg/m^3
L	0.6960-1.0531	m
k_1/k_2	$(2.9389-4.1104) \times 10^{-3}$	-

6.5.2. Comparison with Literature Data

In this part, the numerical results derived for exit solute concentration with the proposed method are compared with the technique of CHCM used by Mittal et al. (2013). The solution profiles are obtained for the exit solute concentration using QHCM with different parameters. The numerical results obtained are tabulated in Table 6.16. The results are derived for Pe=1,10 &40 for division of domain into 20, 40 & 80 elements. It can be noticed from Table that the concentration of solute at exit level with the QHCM is decreasing with time in comparison to the CHCM used by Mittal et al. (2013). The results confirm that the exit solute concentration profiles are converging to the steady-state condition with an increase in Pe and partitions of the domain for different values of Pe. It is also noted that improved washing can be attained for Pe=40. In this regard, Al-Jabari et al. (1994) have exhibited an optimum scale of Pe to be less than or equal to 40.

6.5.3 Comparison in Terms of Number of Elements

The nonlinear model is solved with QHCM for Pe=40 and the experimental data by Arora et al. (2006) is used to validate the numerical results. Ganaie et al. (2014) solved numerically this model for Pe=40 by using the technique CHCM. In this part, the results obtained using the QHCM are compared with the previously published result of Ganaie et al. (2014). The numerical results using QHCM are derived for the partition of the domain into M=50 and 100 elements. Ganaie et al. (2014) derived the results for the partition of the domain into M=100,200 and 300 elements and results are presented in Table 6.17. It is noticed that the results obtained using QHCM by dividing the domain into 50 elements are the same as the results for 100 elements with CHCM. Also, the results obtained using QHCM by dividing the domain into 100 elements are the same as the results for 300 elements with CHCM. This proves that we can derive better results with less number of equations. So, the computational cost is reduced with the present technique.

Table 6.15 Numerical results of concentration of solute at exit level using QHCM for nonlinear model with different range of *Pe* and M

Time	*Pe* =1			*Pe* =10			*Pe* =40		
	M = 20	M = 40	M= 80	M = 20	M = 40	M = 80	M = 20	M = 40	M = 80
0	1.000E+00	1.000E+00	1.000E+00	1.000E+00	1.000E+00	1.000E+00	1.000E+00	1.000E+00	1.000E+00
0.2	9.101E-01	9.209E-01	9.251E-01	1.000E+00	1.000E+00	1.000E+00	1.000E+00	1.000E+00	1.000E+00
0.4	7.423E-01	7.532E-01	7.584E-01	9.791E-01	9.831E-01	9.843E-01	1.000E+00	1.000E+00	1.000E+00
0.6	5.980E-01	6.076E-01	6.115E-01	8.582E-01	8.696E-01	8.741E-01	9.891E-01	9.916E-01	9.922E-01
0.8	4.813E-01	4.891E-01	4.927E-01	6.593E-01	6.739E-01	6.806E-01	8.509E-01	8.651E-01	8.721E-01
1.0	3.887E-01	3.940E-01	3.972E-01	4.624E-01	4.750E-01	4.813E-01	5.384E-01	5.608E-01	5.717E-01
1.2	3.138E-01	3.186E-01	3.203E-01	3.061E-01	3.151E-01	3.201E-01	2.526E-01	2.684E-01	2.762E-01
1.4	2.533E-01	2.578E-01	2.594E-01	1.940E-01	2.017E-01	2.047E-01	9.141E-02	9.902E-02	1.031E-01
1.6	2.051E-01	2.081E-01	2.090E-01	1.207E-01	1.243E-01	1.263E-01	2.720E-02	2.990E-02	3.134E-02
1.8	1.650E-01	1.689E-01	1.691E-01	7.271E-02	7.538E-02	7.669E-02	7.032E-03	7.801E-03	8.201E-03
2.0	1.344E-01	1.360E-01	1.379E-01	4.343E-02	4.512E-02	4.591E-02	1.633E-03	1.831E-03	1.930E-03
2.2	1.083E-01	1.105E-01	1.103E-01	2.575E-02	2.671E-02	2.724E-02	3.511E-04	3.948E-04	4.177E-04
2.4	8.741E-02	8.873E-02	8.937E-02	1.510E-02	1.577E-02	1.601E-02	7.118E-05	8.033E-05	8.514E-05
2.6	7.079E-02	7.171E-02	7.228E-02	8.874E-03	9.214E-03	9.381E-03	1.385E-05	1.562E-05	1.668E-05
2.8	5.721E-02	5.807E-02	5.844E-02	5.181E-03	5.382E-03	5.485E-03	2.570E-06	2.920E-06	3.111E-06
3.0	4.624E-02	4.690E-02	4.721E-02	3.013E-03	3.139E-03	3.192E-03	4.672E-07	5.321E-07	5.660E-07

Table 6.16 Comparison of solution using QHCM and CHCM with input parameters

$C_0 = 0.278; A_0 = 0.01195; B_0 = 2.708; C_s = 0.000; e = 0.942; C_F = 106.9$

		QHCM	CHCM	QHCM	CHCM	QHCM	CHCM
h	**Time**	**Pe =1**		**Pe =10**		**Pe=40**	
0.05	0.6	6.463E-01	6.608E−01	9.104E-01	9.235E−01	9.969E-01	9.982E−01
	1.2	3.807E-01	3.909E−01	4.596E-01	4.779E−01	5.330E-01	5.601E−01
	1.8	2.309E-01	2.382E−01	1.809E-01	1.889E−01	9.292E-02	1.052E−01
	2.4	1.432E-01	1.472E−01	6.277E-02	6.515E−02	7.076E-03	7.214E−03
	3.0	8.929E-02	9.141E−02	2.047E-02	2.075E−02	2.689E-04	2.691E−04
0.025	0.6	6.559E-01	6.633E−01	9.188E-01	9.252E−01	9.975E-01	9.983E−01
	1.2	3.864E-01	3.922E−01	4.705E-01	4.800E−01	5.478E-01	5.635E−01
	1.8	2.354E-01	2.390E−01	1.860E-01	1.899E−01	1.007E-01	1.064E−01
	2.4	1.460E-01	1.476E−01	6.482E-02	6.554E−02	8.245E-03	7.330E−03
	3.0	9.075E-02	9.170E−02	2.118E-02	2.088E−02	4.184E-04	2.741E−04
0.012	0.6	6.608E-01	6.645E−01	9.230E-01	9.261E−01	9.979E-01	9.984E−01
	1.2	3.887E-01	3.929E−01	4.755E-01	4.811E−01	5.590E-01	5.653E−01
	1.8	2.344E-01	2.394E−01	1.885E-01	1.905E−01	1.027E-01	1.071E−01
	2.4	1.443E-01	1.479E−01	6.574E-02	6.574E−02	7.867E-03	7.389E−03
	3.0	8.993E-02	9.184E−02	2.150E-02	2.095E−02	2.739E-04	2.751E−04

Table 6.17 Comparison of solution using QHCM and CHCM with input parameters

$C_0 = 8.33; A_0 = 0.00052; B_0 = 0.000625; C_s = 0.005; e = 0.96; C_F = 66.17$

Time	QHCM		CHCM		
	M=50	**M=100**	**M=100**	**M=200**	**M=300**
0.0	1.0000E+0	1.0000E+0	1.0000E+0	1.0000E+0	1.0000E+0
0.2	1.0000E+0	1.0000E+0	1.0000E+0	1.0000E+0	1.0000E+0
0.4	9.9998E-01	9.9998E-01	9.9998E-01	9.9999E-01	9.9999E-01
0.6	9.8525E-01	9.8653E-01	9.8629E-01	9.8693E-01	9.8714E-01
0.8	8.0515E-01	8.1270E-01	8.1098E-01	8.1476E-01	8.1602E-01
1.0	4.4102E-01	4.5008E-01	4.4752E-01	4.5204E-01	4.5354E-01
1.2	1.6522E-01	1.7011E-01	1.6848E-01	1.7092E-01	1.7173E-01
1.4	4.6837E-02	4.8517E-02	4.4788E-02	4.8723E-02	4.9004E-02
1.6	1.0931E-02	1.1373E-02	1.1182E-03	1.1404E-02	1.1428E-02
1.8	2.2251E-03	2.3255E-03	2.2752E-03	2.3239E-03	2.3401E-03
2.0	4.1062E-04	4.3121E-04	4.1935E-04	4.2879E-04	4.3195E-04

6.5.4 CPU Time Consumed in the Whole Process

The CPU time used for the whole process for a range of Pe is presented in Table 6.18. The results are derived for different partitions of the domain. The CPU time is considered in all cases for $Pe=1,10,40,100$ by dividing the domain into 20,40 and 80 elements. It is depicted that the CPU time is lying between 1.001 to 1.815 seconds. Also, the least CPU time for $Pe=1$; N=20 is 1.001 seconds, and the CPU time for $Pe=1$; N=80 is 1.815 seconds. Although the CPU time is increasing when the domain is partitioned into more elements, however, the results are derived with comparatively less CPU time and not much effect of this is observed with the increase in Pe.

Table 6.18 CPU time (in a sec) for the concentration of solute by dividing the domain into different elements

	$Pe = 1$	$Pe = 10$	$Pe = 40$	$Pe = 100$
Length of each subinterval (h)	QHCM	QHCM	QHCM	QHCM
0.05	1.001	1.007	1.033	1.038
0.025	1.142	1.147	1.113	1.115
0.0125	1.815	1.631	1.658	1.545

6.5.5 Effect of the Division of the Domain

Generally, when the domain is partitioned by adding more points or when the number of elements is increased, better results are observed in solution profiles. The concentration profile results for $Pe=40$ by division of domain into different elements are presented in Figure 6.15. The concentration profile for $Pe=32,64,128$ and 256 overlaps. In other words, when the domain is divided into more than 30 elements, the results for concentration profiles are identical and the breakthrough curves coincide. Hence, using the present method, no more effect of an increase in elements is seen when the elements are increased. It supports that we can derive the results for solution profile with the fewer equation that reduces the mathematical complexity, time, and effort. It proves that we can derive the results with a minimum number of equations using QHCM. Hence, the mathematical complexity is reduced in this technique.

6.5.6 Rate of Convergence and Comparison with CHCM

In this part, the expression used to find the rate of convergence is taken from Farrell and Hegarty (1991) as discussed in chapter 3. To prove the efficiency of QHCM over CHCM, the rate of convergence of both techniques is calculated. The comparison of the rate of convergence for different ranges of Pe from 1 to 300 is presented in Table 6.19. It is seen from this table that the rate of convergence using the present method is noticed to be nearer to one than the previous technique CHCM. Also, it can be observed that QHCM gives a better result for the rate of convergence than CHCM. So, the efficiency of the method is proved.
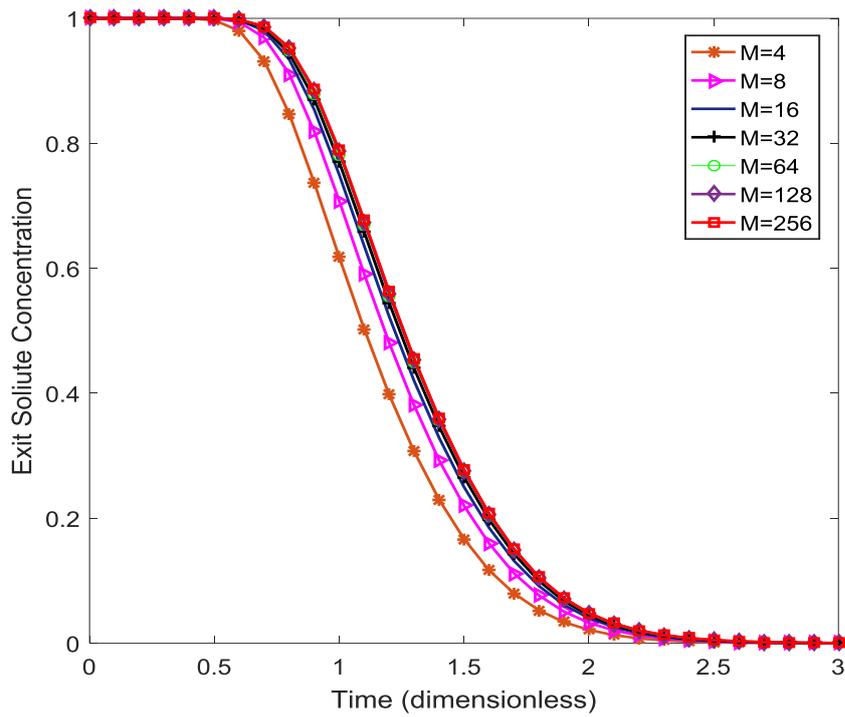
Figure 6.15 Exit solute concentration profile for *Pe*=40 for division of domain into different elements

Table 6.19 Comparison of rate of convergence of CHCM and QHCM

M	Pe=1		Pe=10		Pe=20	
	QHCM	CHCM	QHCM	CHCM	QHCM	CHCM
2	0.948079	0.948127	1.026624	1.013162	1.190028	1.173365
4	1.014312	0.968717	0.983575	0.888302	1.085259	0.902669
8	0.973431	0.978063	0.984443	0.915241	0.936818	0.865635
16	1.006082	0.993243	1.056620	0.949505	1.056206	0.911152
32	1.015682	0.994233	0.976189	0.972693	0.945633	0.943669
M	Pe=40		Pe=100		Pe=300	
	QHCM	CHCM	QHCM	CHCM	QHCM	CHCM
2	1.185371	1.183820	1.016121	0.962791	0.898063	0.721321
4	1.021715	1.111741	1.137504	1.330525	0.976559	0.971066
8	1.003269	0.807817	1.014903	1.076677	1.166885	1.463702
16	0.989565	0.846704	0.985348	0.734532	1.222787	1.302781
32	0.902025	0.904348	0.930329	0.796253	1.014869	0.569730

6.5.7 Effect of *Pe* on Concentration Profiles

The behavior of solution profiles for exit solute concentration with different parameters is shown by breakthrough curves. The Pe which is the ratio of advection to diffusion is mainly considered a basic factor to describe the behavior of displacement washing. (Makinde and Animasaun, 2016). It is therefore affected by the diffusion coefficient. The advection dominate diffusion in the case of *Pe*>1 and diffusion dominate advection in the situation when *Pe* is less than 1. Jannesari and Tatari (2020) suggested that to avoid the situation of oscillatory numerical solutions the choice of these parameters plays an important role in the discretization process. These parameters should be chosen according to the need to attain stability.

The outcomes of exit solute concentration are expressed as breakthrough curves for a wider range of Pe varying from lower to higher. The concentration profiles at the exit level approach steady-state condition with the increase in time. The solution profiles for small Pe are presented in Figure 6.16. It is noticed from the figure that concentration profiles are vertiginous when Pe is very small and, in this situation, much time is taken by solute to come out from the pores of particle. This happens because diffusion plays a leading role for a small value of *Pe* whereas the interstitial velocity is small, and the concentration profiles reach the situation of slow convergence. Further, as *Pe* is close to zero, the axial dispersion coefficient is noticed to be increasing followed by a rise in the back mixing effect whereas, the cake thickness and interstitial velocity remained constant. It is also observed that in this state, the value of added fluid quickly mixes with pulp and the same amount of black liquor is discharged from the pulp. This is a case of perfect mixing.

Perfect mixing: Arora et al. (2006) explained that this is a situation when *Pe* is negligible, or *Pe* is nearer to 0 because the axial dispersion coefficient is in dominating condition. This is a state when the introduced solvent immediately mixes up into the bed through the bed and the fluid comes out by an equal amount from the bed. The time taken by solute to diffuse out becomes indefinitely large due to the rapid increase in D_L. Further, the effect of large *Pe* on concentration profiles is depicted in Figure 6.17. It is noticed that when the value of *Pe* is increased, the washing time decreases steeply. It specifies that a large value of *Pe* will make the axial dispersion coefficient smaller, and more solute will dispense from the pores of the particle. This is a state when the original

contents from the bed are enforced to get out as a piston-like style when the displacing fluid is introduced. This is a case of perfect displacement (Pouteck,1997).

Perfect displacement: This is a situation when Pe is indefinitely large, or Pe approaches infinite value, and the dispersion coefficient is close to zero. In this case, the contents initially attached to the pulp bed are forced out in a piston-like fashion by the displacing liquid. Moreover, when Pe increases, the concentration at the exit level approaches to steady state condition more rapidly with time.

In an ideal situation, the soluble impurities lying within the pulp washing bed cannot be properly removed. Although the medium range of Pe is preferred because more time is taken by the residing solute to wash out and concentration profiles are slowly converging to zero, this is the case of quite an acceptability. Hence, the industries need an optimum scale of Pe to keep up a balance between the washing time and omission of impurities (Potůček, 1997). Al-Jabari et al. (1994) demonstrated that better washing is attained for an optimum scale of Pe between 30 and 50. The study supported that the choice of Pe mainly affects the washing process. Practically, the industry must maintain parity among the exclusion of impurities and washing time. Further, it was also exhibited that flow characterization of pulp fiber-packed beds can be better illustrated by $Pe = 40$. Figure 6.18 signifies that the results attained using QHCM for a parameter with a medium range are proved to be true in the study. The optimum washing is achieved in this situation. It can be observed from the figure that the solute concentration at the exit level is best described for the value of Pe having a medium range. In this regard, Jannesari and Tatari (2020) also explained the exit solute concentration profile for this range.

6.5.8 Influence of D_L on the Concentration

The axial dispersion coefficient plays a prominent role in the washing of pulp fibre bed process which is inversely proportional to Pe. Carrara et al. (2003) experimentally estimated the axial dispersion coefficient (D_L) which affects the output results. Jiwari et al. (2018) explained an extensive range of solution profiles affected by a wide range of diffusion coefficients.

The effect of D_L is studied for the nonlinear model and presented in Figure 6.19. The role of diffusion is prominent in the pulp washing process when the value of D_L is more. It is noticed from the figure that an increase in D_L rises the level in back mixing and

black liquor solute removal is reduced. Due to this fact, the solute adsorbed on fiber surface remains attached and also needs more time to remove which makes the washing process improper. In this situation, the solution profile converges slowly. Also, the figure depicted that when the value of D_L decreases and the value of Pe increases, the washing efficiency increases. In the case of small D_L, the solute (black liquor) was removed in a better way due to less back mixing. It results in increasing washing efficiency. So small value of D_L improves washing and makes the washing operation effective. The studies of Gupta et al. (2015), and Kukreja and Ray (2009) also supported this result.

6.5.9 Influence of *u* on Concentration

The velocity index also lies in the category of important factors which generally affect the solute concentration (Animasaun et al., 2019). It is directly proportional to the *Pe*. The increase in interstitial velocity causes an increase in *Pe* and this diminishes the effect of diffusion of solute from the pores of the particle. Also, the rate of increase in u is governed by the bed porosity and particle geometry (Trinh et al., 1989). Carrara et al. (2003) proved that the most common state in a tabular reactor happens for the range of *Pe* from 20 to 100 and it also depends on superficial velocity. The study also revealed that the experimental behavior of plug-flow models can be predicted with high accuracy by the specific range of these parameters.

The effect of interstitial velocity on the pulp washing curve is expressed in Figure 6.20. It illustrates that velocity does not significantly affect the shape of the washing curve. Potůček (1997) also supported this fact and observed the linear relation between D_L and *u*. While the studies of Lee (1979); Sridhar (1999) have shown that with the introduction of little flow of fluid the black liquor is easily removed as compared to the high flow. On the other hand, the overall interstitial velocity on account of an increase in axial dispersion does not affect the concentration profiles.
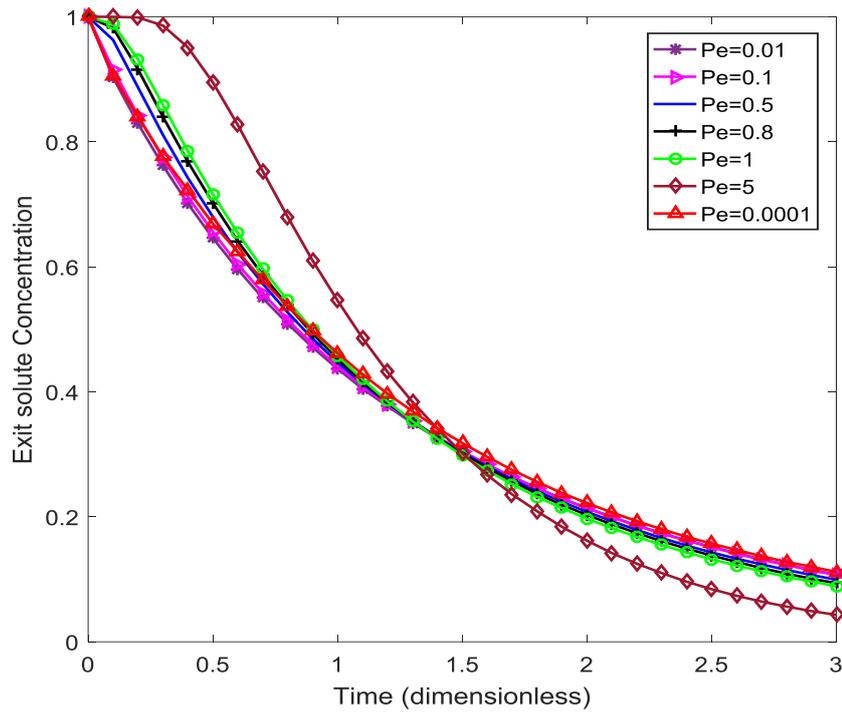
Figure 6.16 Influence of small value of *Pe* on the concentration profile
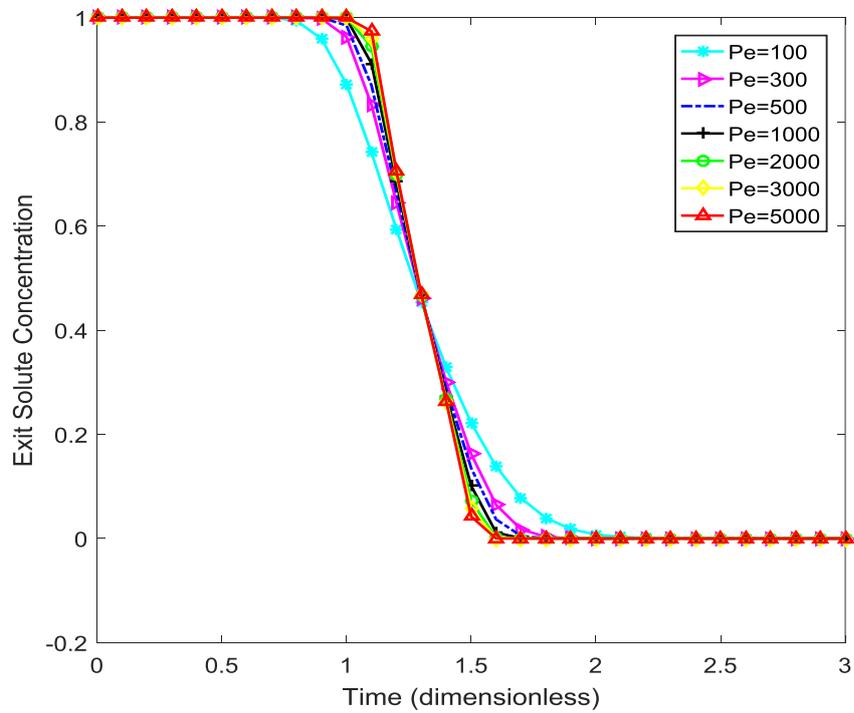
Figure 6.17 Influence of large value of *Pe* on the concentration profile
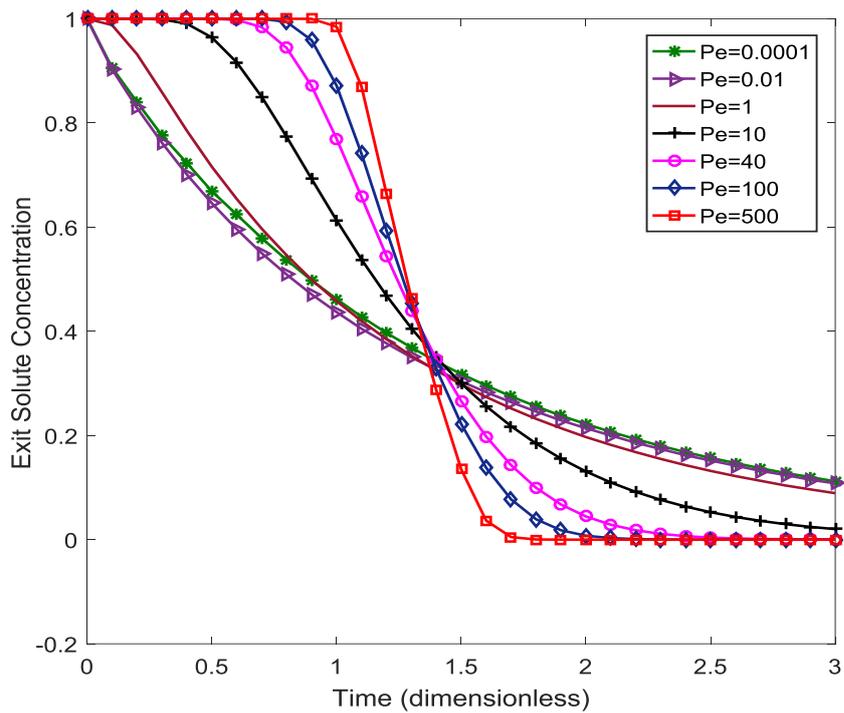
Figure 6.18 Influence of *Pe* on exit solute concentration
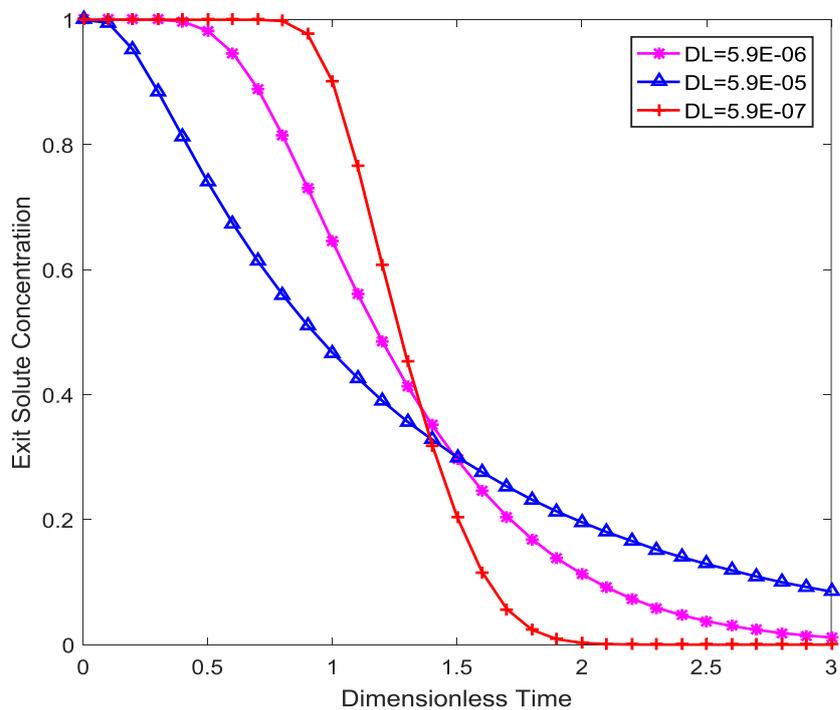
Figure 6.19 Influence of D_L on concentration profiles for *u*=4.0E-03 and *L*=0.02.
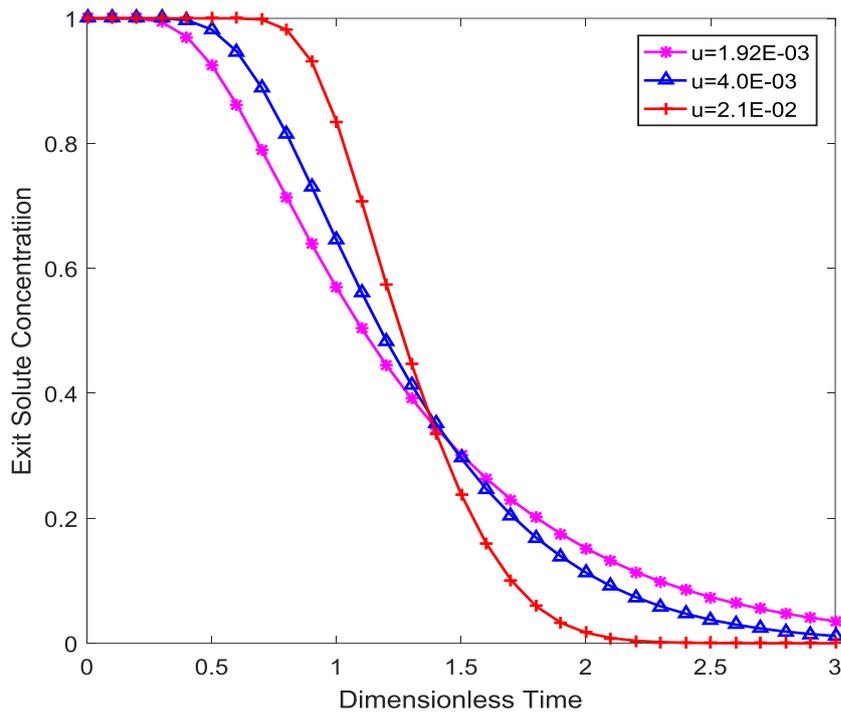
Figure 6.20 Influence of *u* on concentration profile for *L*=0.02 and D_L =5.9E-06

6.5.10 Effect of L on the Concentration

As discussed by Sharma et al. (2018), the concentration of fluid is significantly affected by some other important parameter such as cake thickness. The thickness of the cake influences the concentration profiles when the *Pe* is high. This effect of change in cake thickness is illustrated in Figure 6.21. The figure shows the decrease in breakthrough time when the value of *L* is slightly increased from 0.02cm, but the concentration profiles are found to be overlapped when the value of *L* is increased from 0.04 cm. Hence, better washing can be attained when the cake thickness is increased because more value of *L* enables more amount of solute to disperse out from the pores of the cake. Lee (1979); Arora et al. (2006); Mittal et al. (2013) also concluded that similar consequences of cake thickness.
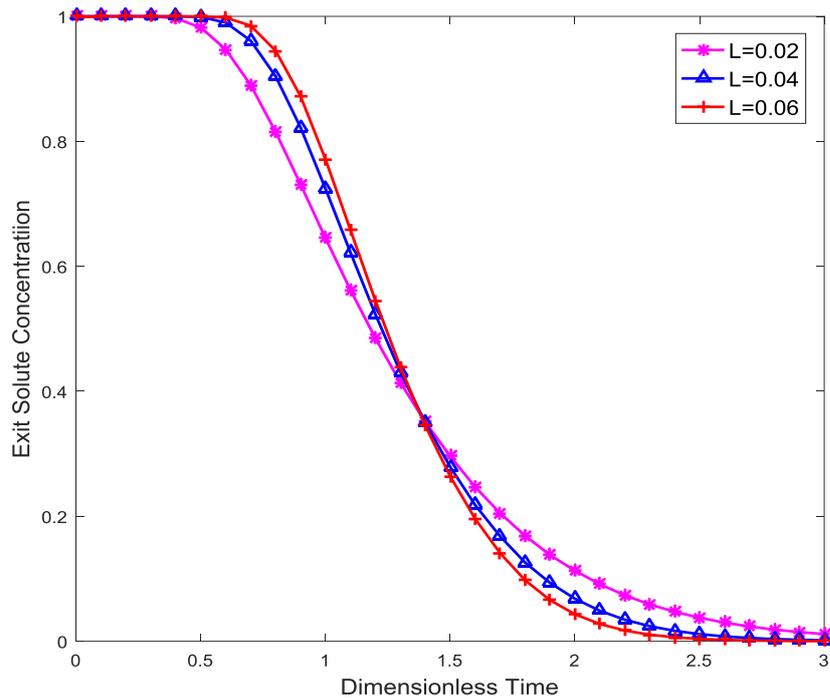
Figure 6.21 Influence of *L* on concentration when *u*=4.0E-03 and D_L =5.9E-06.

6.5.11 Effect of Bed Porosity

The porous nature of the pulp fiber bed is an essential factor in the washing procedure. Although washing operation is mainly influenced by *Pe*, yet the porosity is another parameter that influences the flow, and the washing process. This depends on the geometry of the packed bed (Augier et al., 2010). Potůček (1997) explained that the type of pulp or fiber characteristics is the main variable that affects the dispersion coefficient. Despite this, the average pore size, difference in geometry and pore size distribution that occurs in fiber material have an effect of dispersion in the pulp bed. The effect of porosity on the concentration of solute at the exit level is described in Figure 6.22. In the case of high porosity, the fiber surface absorbs more solute, and this can help to achieve the target of washing with less amount of water. Moreover, this is also a situation when the removal rate of impurities is more from the fiber surface with less time in the case when the porosity level is significantly large. This result is also supported by Arora et al. (2006).
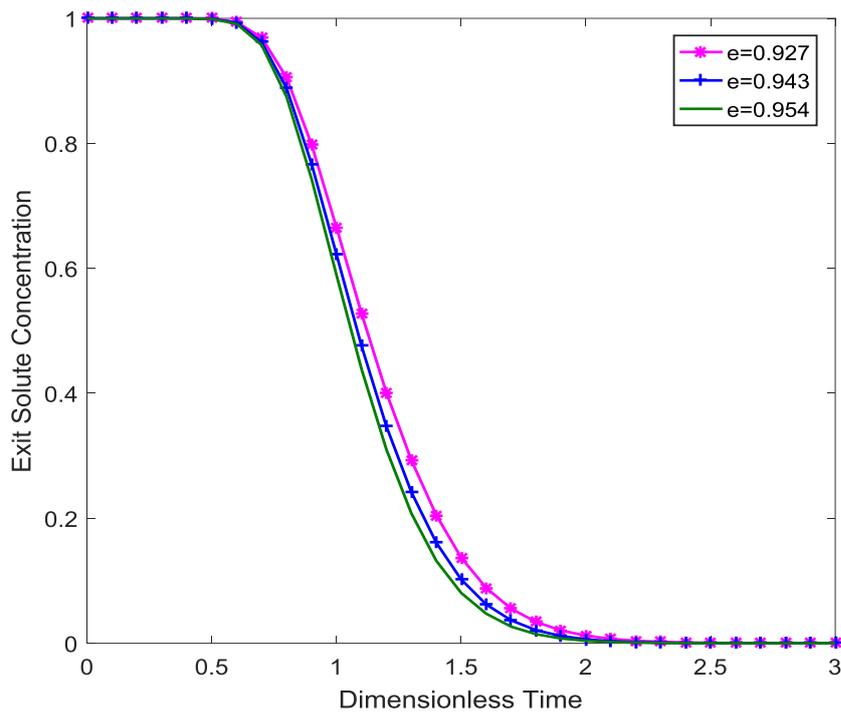
Figure 6.22 Influence of porosity on concentration profile.

6.5.12 Surface Plot Representation

The surface plot performs an important role to simulate the physical behavior of packed bed solute concentration at exit level for any location for the time more practically and prospectively. The surface plot for the nonlinear model with *Pe*=1,10,40,300 is presented in Figures 6.23-6.26. Figure 6.23 and 6.24 indicates that for small *Pe*, the adsorbed solute on the fiber surface needs more time to detach from the fiber surface because small *Pe* makes more dispersion of solute due to this more back mixing occurs. It is also noticed from Figure 6.26 that improper washing is seen for very large *Pe*. Moreover, it is noted that the surface plot for *Pe*= 40 shows a better washing curve as in Figure 6.25.
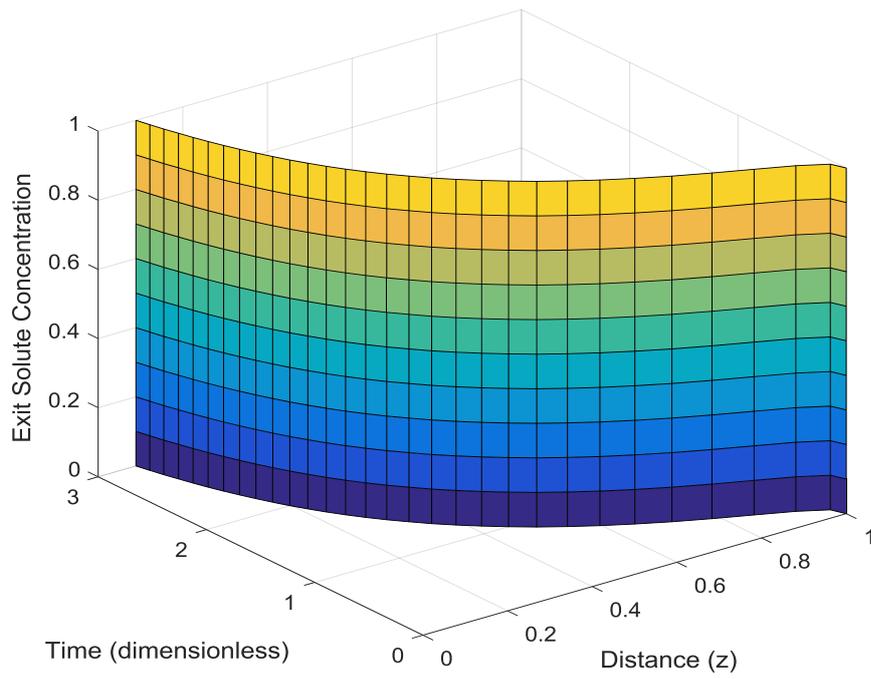
Figure 6.23 Surface plot for non-linear model for *Pe*=1
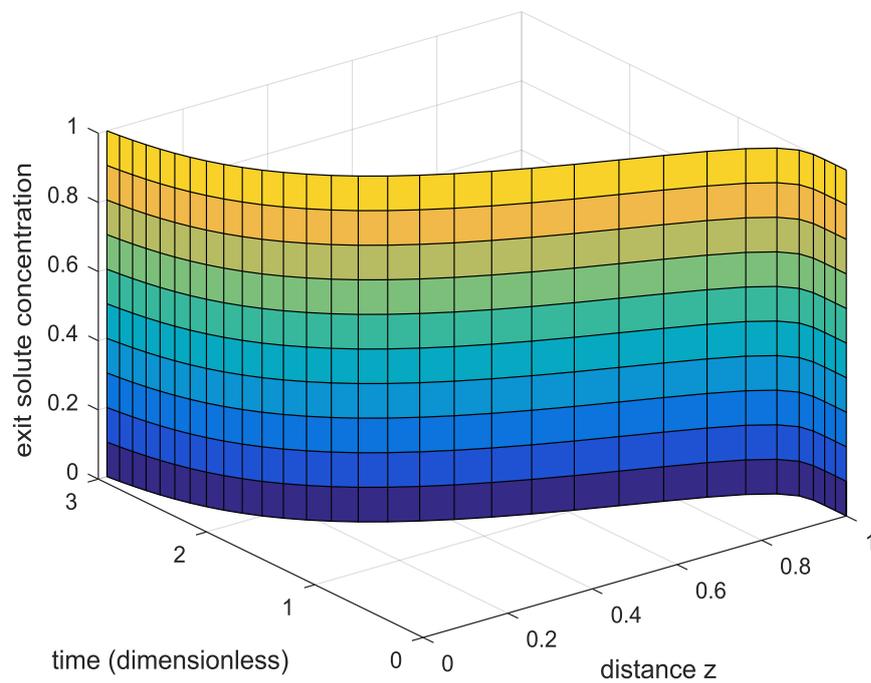
Figure 6.24 Surface plot for non-linear model for *Pe*=10
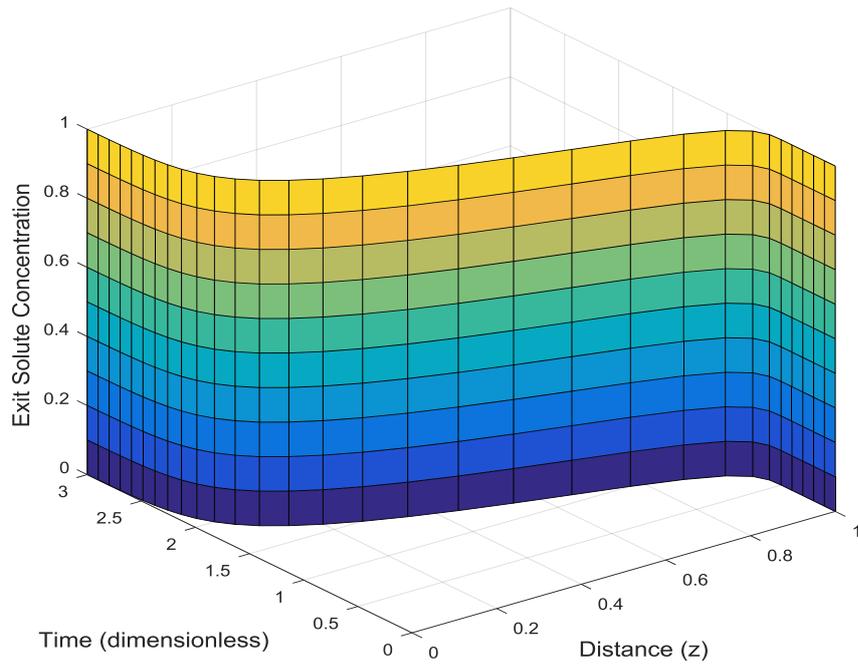
Figure 6.25 Surface plot for non-linear model for *Pe*=40
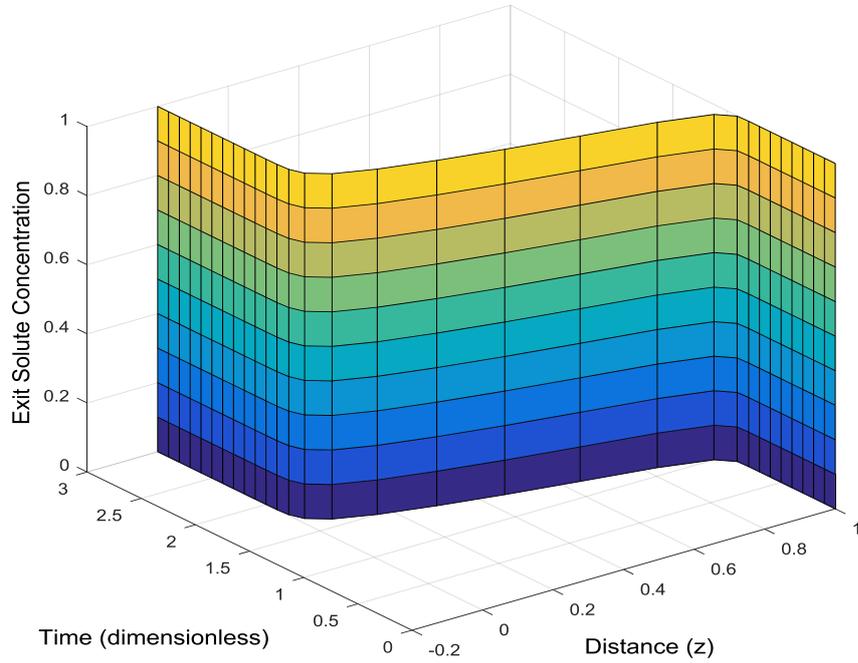
Figure 6.26 Surface plot for the non-linear model for *Pe*=300

6.5.13 Relation with the Industrial Parameters

The performance of the pulp washing process in the paper industry is examined by the amount of black liquor(impurities) removed. High effectiveness of the washing process can be attained when a large amount of impurities adsorbed on the surface of fiber are removed in a short period. In this work, the industrial parameters connected with the concentration of solute which are commonly used such as bed efficiency and displacement ratio are mathematically estimated.

Displacement ratio (DR)

The displacement ratio is a common performance parameter used in the industry. It indicates the actual decrease of effluent liquor relative to the maximum possible decrease (Kukreja, 1996) and is defined as:

$$DR = \frac{c_0 - c_d}{c_0 - c_s}$$

where c_0 is initial solute concentration, c_s is the solute concentration in wash liquor, and c_d is the average solute concentration.

The effect of DR for different Pe in the form of a breakthrough curve is shown in Figure 6.27. It is observed that for the large value of Pe, more quantity of black liquor is removed because the dispersion is small in this case. Due to this, less back mixing occurs, and the impurities adsorbed on fiber are removed in large quantities in a short time interval. When the value of DR is 1, the 100% solids are assumed to be removed from the packed bed, although it is not possible in a real sense. Thus, for the high value of Pe, maximum reduction of dissolved solids is possible and better washing can be achieved. Arora and Potůček, (2012) and Mittal et al. (2013) have also supported this result by solving the model with OCFE and CHCM respectively.

Bed efficiency (E)

During the washing operation, the change in the amount of effluent liquor is described by bed efficiency. Efficiency is determined on the baseis of the quantity of black liquor solids removal (Kukreja et al., 1995) and it is defined as:

$$E = \frac{c_e - c_s}{c_d - c_s}$$

where c_e is exit solute concentration, c_s is solute concentration in wash liquor, and c_d is average solute concentration.

The effect on bed efficiency for a range of *Pe* is shown in Figure 6.28. It is observed from the figure that efficiency is increased with high *Pe* in comparison to small *Pe*. Potůček (1997) described that the bed efficiency is evaluated when the wash liquor ratio is equal to unity. In case, when the wash liquor ratio is increased from 0 to 1, the bed efficiency is increased indefinitely. This is a situation of pure displacement for the existence of perfect plug flow. The concentration of lignin at the outlet for the perfectly mixed vessel is the same as the average concentration inside the bed and the efficiency is equal to unity in this case. In the ideal situation, bed efficiency lies in the range from 1 to infinity. Moreover, the output of the washing operation is also affected by other factors such as particle orientation, pulping process, porosity (porous nature) of the packed bed, type of substance, and time consumed in the washing operation. Mittal et al. (2013) also demonstrated the same result by employing CHCM.

6.5.14 Simulation with Experimental Data

The applicability of the model is checked in the study using actual industrial data taken from a brown stock washer (for pulp washing) at the fourth stage of a paper mill. The solution of the mathematical model with respect to washing zone is derived using the experimental data given by Grähs (1974), Kukreja (1996), and Arora and Potůček (2012). The detailed data of experimental values of the lab-scale drum washer given by these authors are presented in Tables 6.12 to 6.14. Although the available experimental data varies across the paper mills, the only purpose of applying this method is to prove its efficiency in solving the model.

Paper mill 1

Subsequently, the experimental data of Grähs (1974) is used to solve the nonlinear model with QHCM in the present study. The results so derived were found to be better and consumed less CPU time. Further, Arora et al. (2005), Gupta and Kukreja (2012) and Mittal et al. (2013) used the experimental study of Grähs (1974) to solve the model with OCFE, CSCM, and CHCM respectively. All these authors proved their superiority in numerical results with their respective techniques. Besides, in the earlier paragraphs, the numerical results using QHCM are also compared with Mittal et al. (2013) and

solution profiles are noticed to converge fast in less time as compared with the numerical technique used by Mittal et al. (2013). Further, the exit solute concentration profile using experimental data from Grähs (1974) is also presented in the form of a 3D plot in Figure 6.29.

Paper mill 2

In the next phase, the experimental data of Kukreja (1996) is also used as the input parameters to study the present model. Kukreja (1996) performed the lab-scale experiment on a drum washer that is 30.48 cm wide with a diameter of 23.46 cm. The temperature throughout the washing process of pulp (kappa number 20) is 348 K. The nonlinear model is solved with the QHCM using this experimental data and found that the results derived were better than the earlier studies. The behavior of solute concentration using the present method for the nonlinear model in the form of the surface plot is presented in Figure 6.30. Arora et al. (2005) also used this data to solve the nonlinear model with OCFE and attained the results for some parameters like cake L, Pe, and D_L.

Paper mill 3

Arora and Potuček (2012) experimented with a rotary vacuum washer, which is 4.8768m long with a diameter of 5.7912m and fractional submergence of the drum is 40%. The temperature throughout the washing process of pulp (kappa number 15) is 323 K. The experimental data of raw material as wheat straw given in the study is taken as input parameters. Arora et al. (2005) used the OCFE method to solve the nonlinear model in their study. Further, Ganaie et al. (2014) also used this data to solve the nonlinear model with CHCM and proved the superiority of this method. In the present work, the nonlinear model is solved with the QHCM using the data of Arora and Potůček (2012) and the validity of the method is proved. Besides, to substantiate the results, the behavior of solute concentration at the exit level concerning time and distance (cake thickness) is presented as a 3D plot in Figure 6.31.

It is observed from the three surface plots (Figures 6.29 to 6.31) that the concentration of solute at the exit level is decreasing more rapidly with the experimental data of Kukreja (1996) and Arora and Potůček (2006) in comparison with Grähs (1974). The reason may be the difference in parameters such as porosity, and climatic conditions. The dispersion coefficient, interstitial velocity, cake thickness, and difference in initial

solute concentration are also responsible for determining the efficiency of the pulp washing. The results will be advantageous especially to the paper industry as it indicates reducing the environmental load and attaining optimum efficiency.
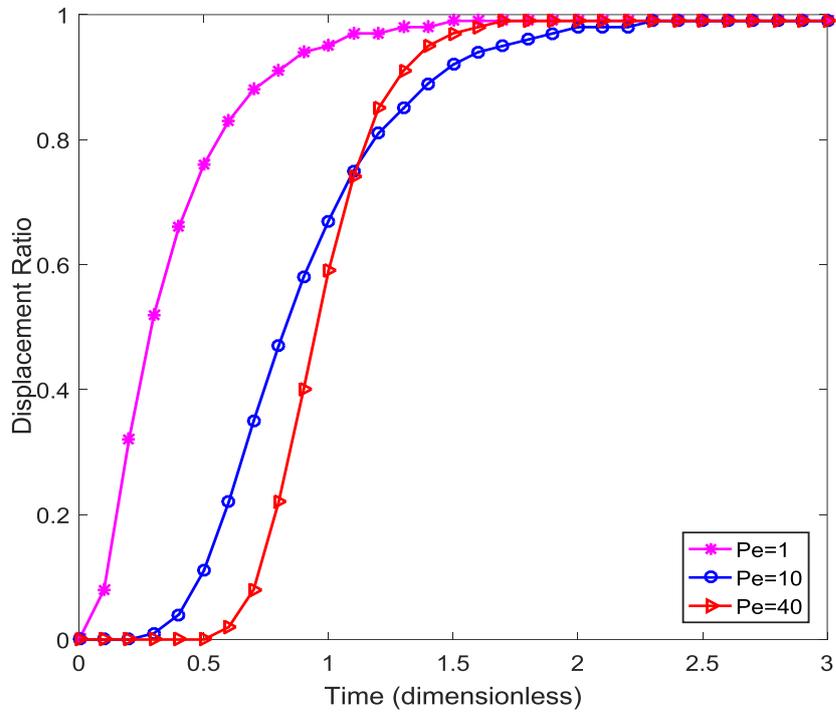
Figure 6.27 Influence of *Pe* on Displacement ratio
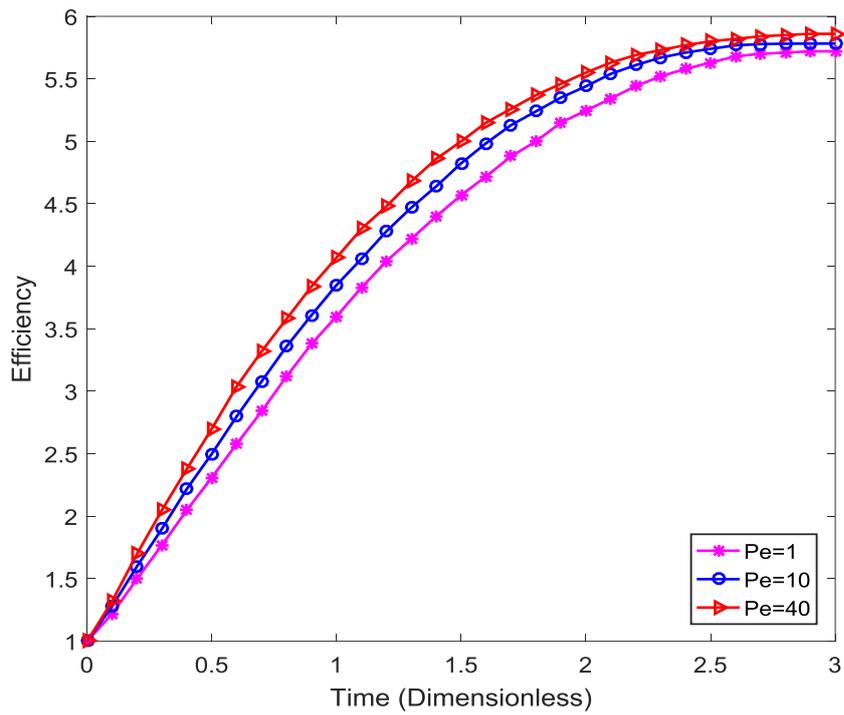
Figure 6.28 Influence of *Pe* on bed efficiency
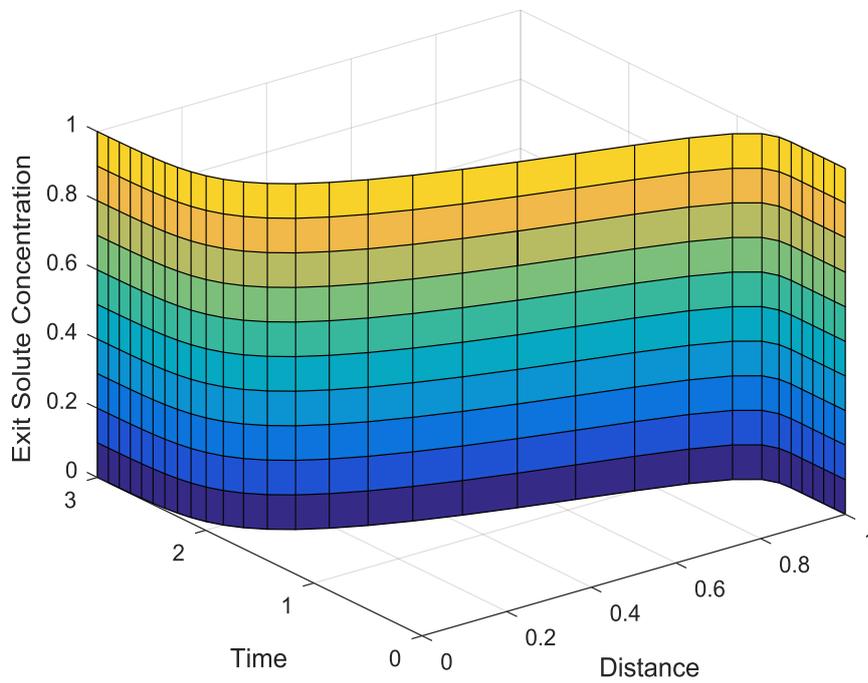
Figure 6.29 3D plot for concentration profile at exit level using experimental data of Grähs (1974)
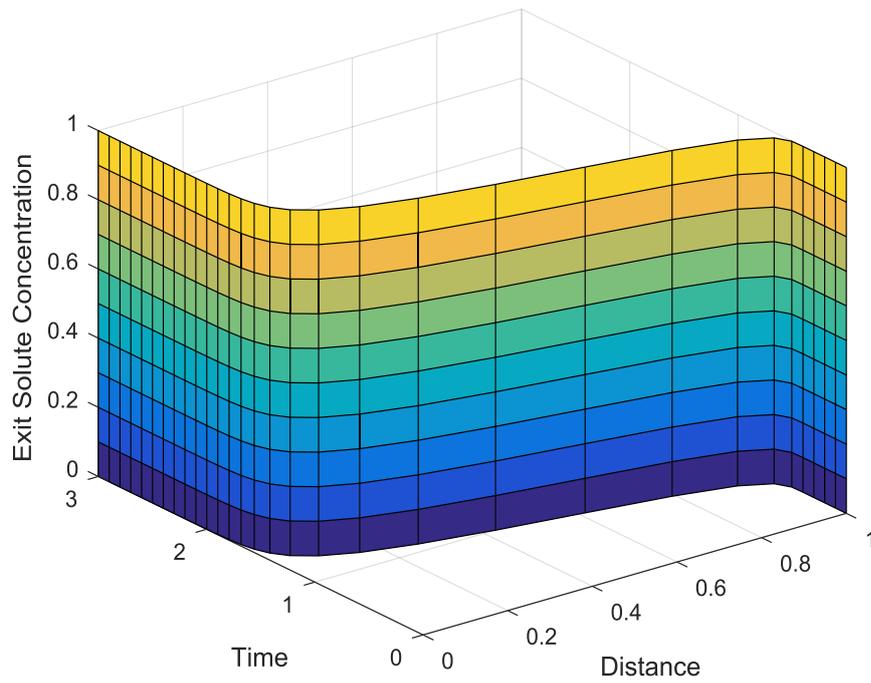
Figure 6.30 3D plot for concentration profile at exit level using experimental data of Kukreja (1996)
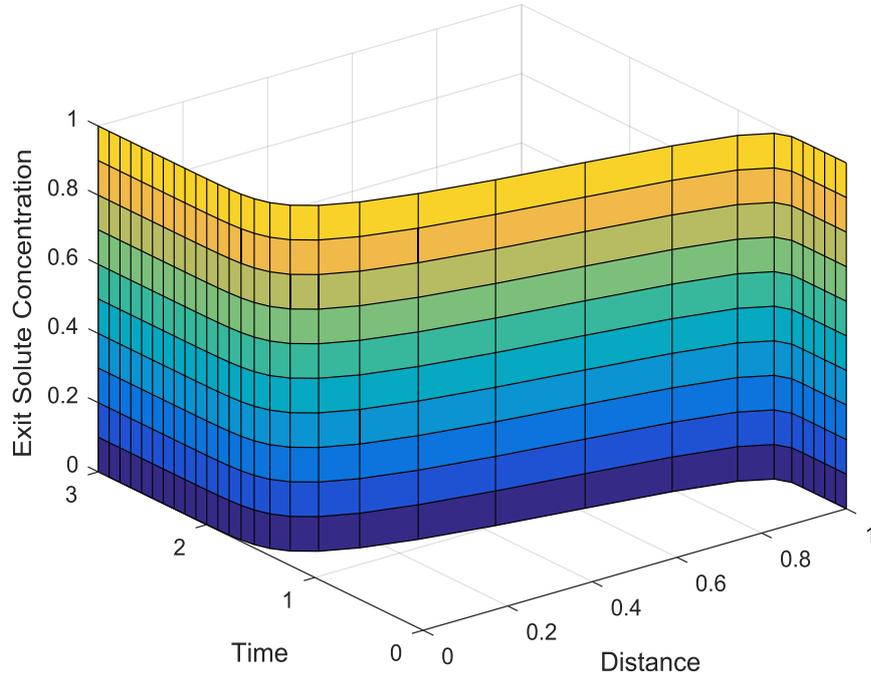
Figure 6.31 3D plot for concentration profile at exit level using experimental data of Arora and Potuček (2012)

6.6 VERIFICATION OF NONLINEAR MODEL-2

The nonlinear model is solved using the QHCM for different values of parameters such as Pe, bed porosity, axial dispersion coefficient, and cake thickness by developing MATLAB codes. The numerical results obtained for this model are verified using the experimental data of Grähs (1974). Mittal and Kukreja (2015) also solved this model by using the technique of CHCM. In this study, the model is solved using QHCM by considering the range of Pe from 1 to 300 and the results are displayed in Table 6.20. The numerical results for Pe=1,10,40 and 300 are also represented by 3D plots from Figures 6.32 to 6.35. It is noticed from the table that the concentration profile at the exit level is decreasing with an increase in time. Initially, the concentration of solute is 1.0 and it started decreasing with time. The deviation in the solution profile is observed for a value of Pe lower than 20 (say 10 to 19) and deviation is minimum in the solution profile with high Pe. Kumar et al. (2009) also supported these results and observed the effects of Pe on the concentration of solute at exit level for sodium ions and lignin ions. Also, the washing is improved with the increase in Pe. This is because the axial dispersion coefficient decreases with an increase in Pe. But when Pe takes very large values then the solution profiles do not give good results and washing is not proper. Roininen and Alopaeus (2011) also favored that the case more increase in Pe show fluctuations that lead to negative concentrations. So, the value of Pe lying in the medium range is preferred to achieve better washing.

Table 6.20 Solution profile for nonlinear model-2 for various values of *Pe*

Time	*Pe* =10	*Pe* =20	*Pe* =40	*Pe* =100	*Pe* =300
0.0	1.000E+0	1.000E+0	1.000E+0	1.000E+0	1.000E+0
0.1	1.000E+0	1.000E+0	1.000E+0	1.000E+0	1.000E+0
0.2	1.000E+0	1.000E+0	1.000E+0	1.000E+0	1.000E+0
0.3	9.985E-01	1.000E+0	1.000E+0	1.000E+0	1.000E+0
0.4	9.859E-01	9.995E-01	1.000E+0	1.000E+0	1.000E+0
0.5	9.493E-01	9.937E-01	9.999E-01	1.000E+0	1.000E+0
0.6	8.860E-01	9.710E-01	9.974E-01	1.000E+0	1.000E+0
0.7	8.041E-01	9.214E-01	9.825E-01	9.995E-01	1.000E+0
0.8	7.142E-01	8.457E-01	9.395E-01	9.933E-01	1.000E+0
0.9	6.244E-01	7.531E-01	8.614E-01	9.609E-01	9.976E-01
1.0	5.399E-01	6.541E-01	7.567E-01	8.758E-01	9.659E-01
1.1	4.630E-01	5.571E-01	6.409E-01	7.427E-01	8.420E-01
1.2	3.944E-01	4.669E-01	5.268E-01	5.924E-01	6.507E-01
1.3	3.340E-01	3.858E-01	4.214E-01	4.501E-01	4.666E-01
1.4	2.815E-01	3.145E-01	3.283E-01	3.253E-01	3.052E-01
1.5	2.361E-01	2.530E-01	2.484E-01	2.198E-01	1.667E-01
1.6	1.973E-01	2.009E-01	1.823E-01	1.353E-01	6.465E-02
1.7	1.642E-01	1.575E-01	1.295E-01	7.422E-02	1.547E-02
1.8	1.361E-01	1.220E-01	8.906E-02	3.653E-02	6.255E-03
1.9	1.125E-01	9.336E-02	5.942E-02	1.767E-02	1.990E-03
2.0	9.277E-02	7.072E-02	3.855E-02	9.484E-03	1.499E-04
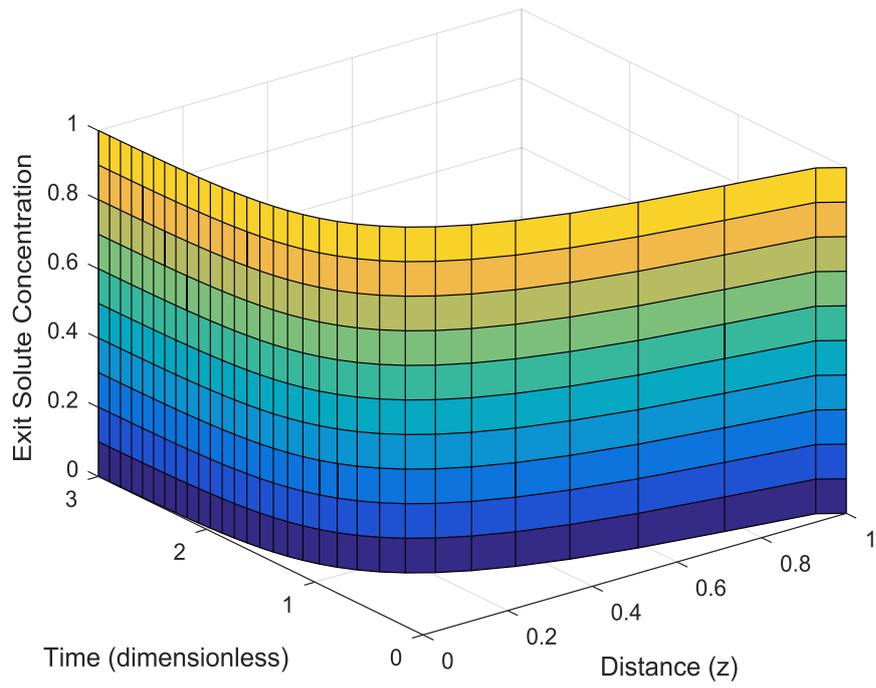
Figure 6.32 3D plot for concentration profile at exit level for *Pe*=1
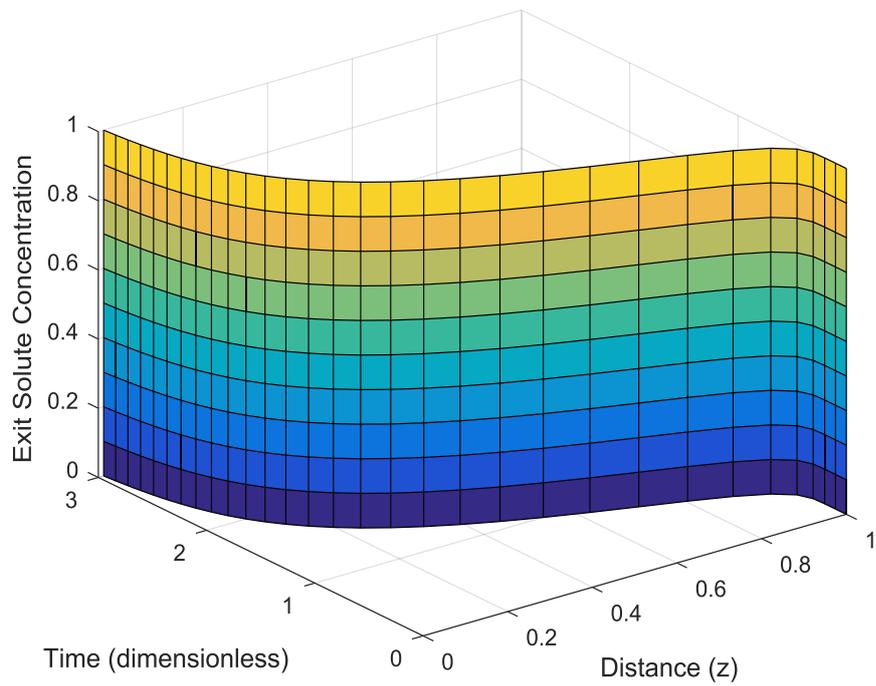
Figure 6.33 3D plot for concentration profile at exit level for *Pe*=10
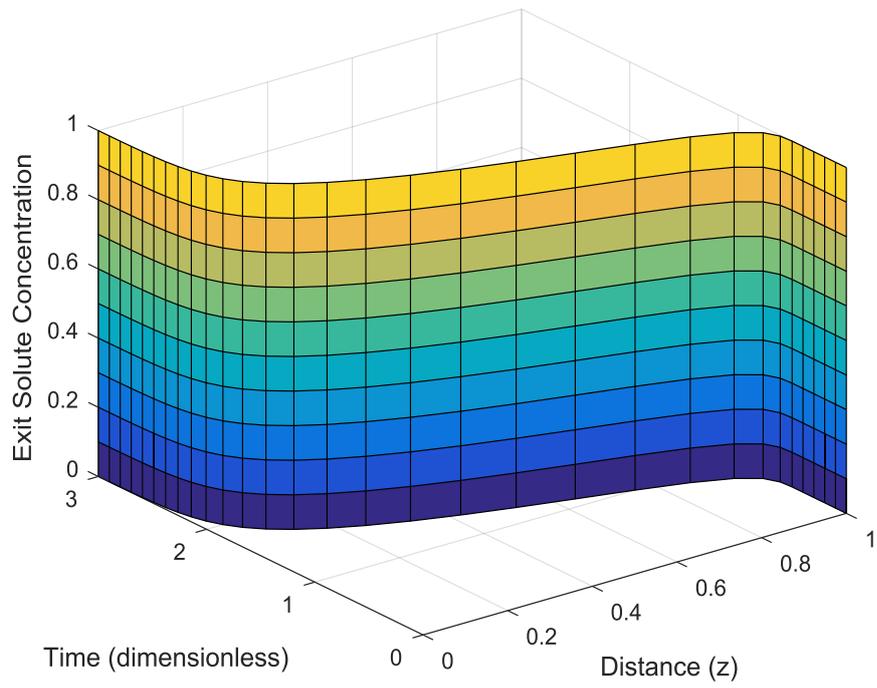
Figure 6.34 3D plot for concentration profile at exit level for *Pe*=40
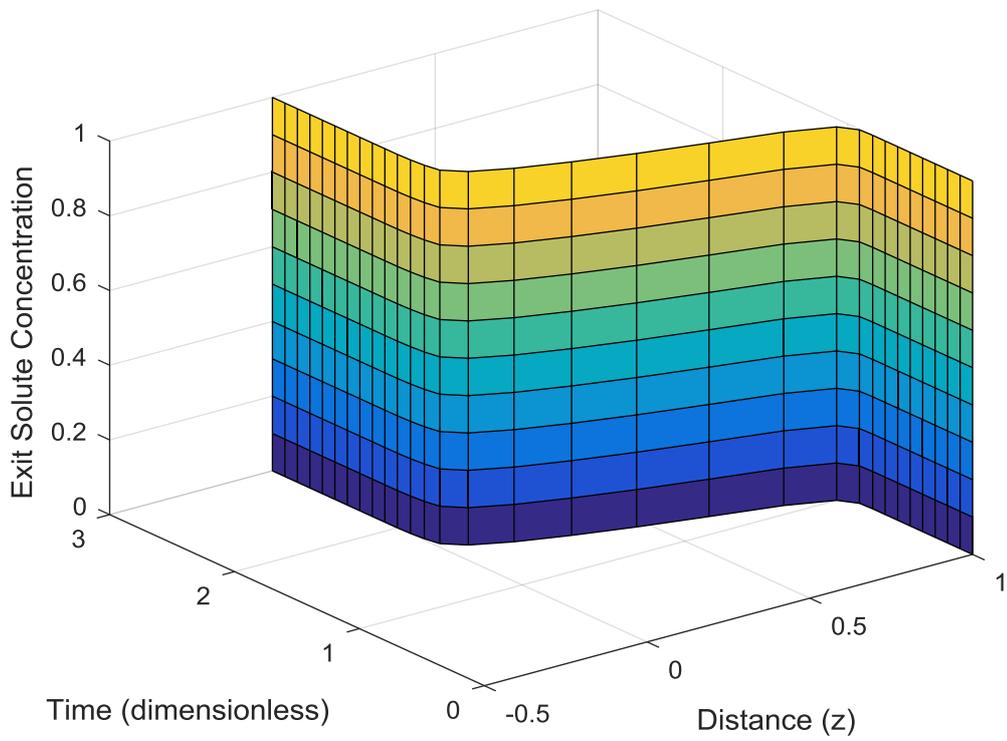
Figure 6.35 3D plot for concentration profile at exit level for *Pe*=300

6.7 COMPARISON OF NONLINEAR MODEL 1 AND 2

The numerical results for exit solute concentration using QHCM for both the nonlinear models are derived in the above discussion. In this part, the numerical results are compared for both models for different values of *Pe*. The experimental data of Grähs (1974) is used to simulate the results. The exit solute concentration is exposed with the breakthrough curves for both models in Figure 6.36. The domain in the case of both models is divided into 40 elements and the results are derived for *Pe*=10,40 and100. The concentration profiles for *Pe* = 40 to 110 are rising at the lower side of the curve and both the models have good agreement. It is noticed from the figure that both the models are giving the same output results when *Pe* is increased from 40 but for *Pe* less than 40 the exit solute concentration for both the models is not providing the same results. Hence, not much considerable difference is observed between the solution profiles for the nonlinear models 1 and 2.
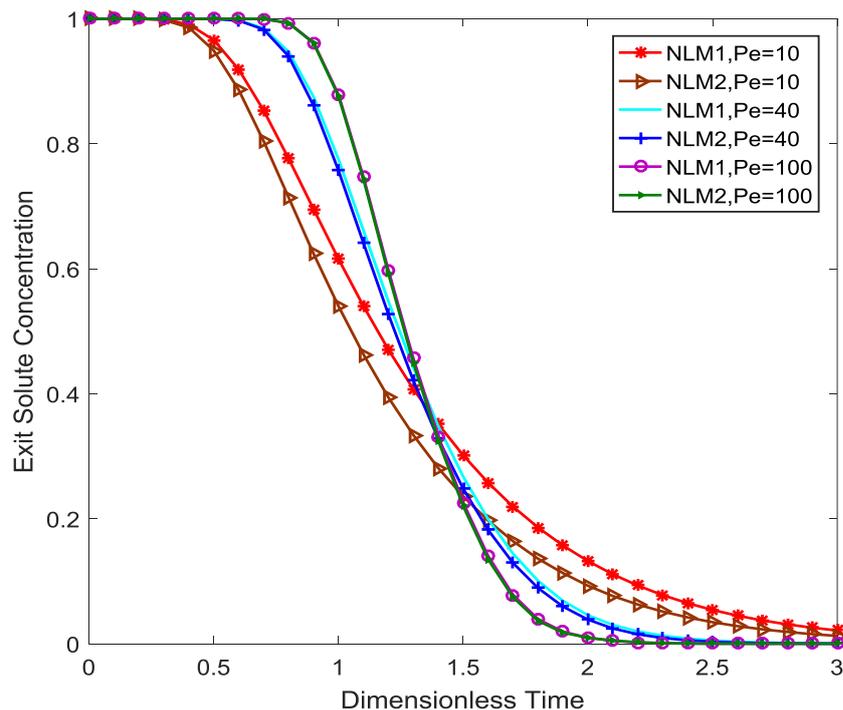
Figure 6.36 Comparison of concentration profile at exit level for nonlinear model-1(NLM1) and nonlinear model-2(NLM2)

6.8 VERIFICATION OF NONLINEAR MODEL-3

The nonlinear model is solved using the QHCM for different values of *Pe*. In this model, linear isotherm is used to describe the connection between solute concentration in liquor and fiber. The model is solved for the division of domain into different elements for *Pe*=10,40 and 100. It is noticed from Figure 6.37 that when the domain is partitioned into 5 elements for *Pe*=10, the solute comes out in a better way as compared to the case for 10 elements. Similarly, the concentration profile at exit level *Pe*=40 with the number of elements 5 provides better results than the division of the domain into 10 elements. But as soon as, the value of *Pe* is increased to 100, the washing results are better with the number of elements 10. Hence, in all cases, we can derive better results with less division of elements, and we need less number of equations than CHCM used by Ganaie et al. (2013). This proves that computational cost and time are reduced with this method.
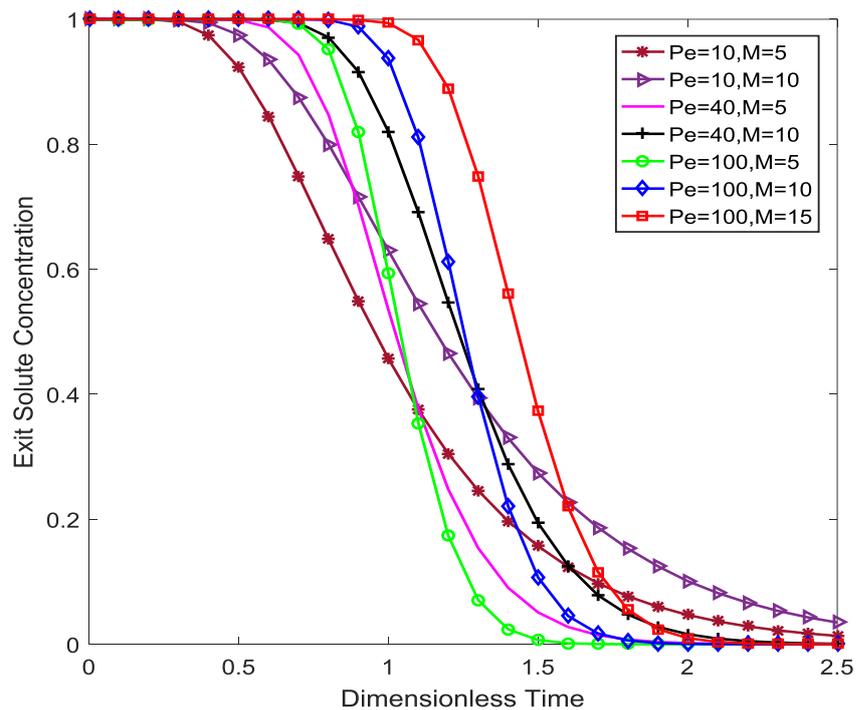
Figure 6.37 Comparison of exit solute concentration profile by division of domain into different elements for *Pe*=10, 40, 100
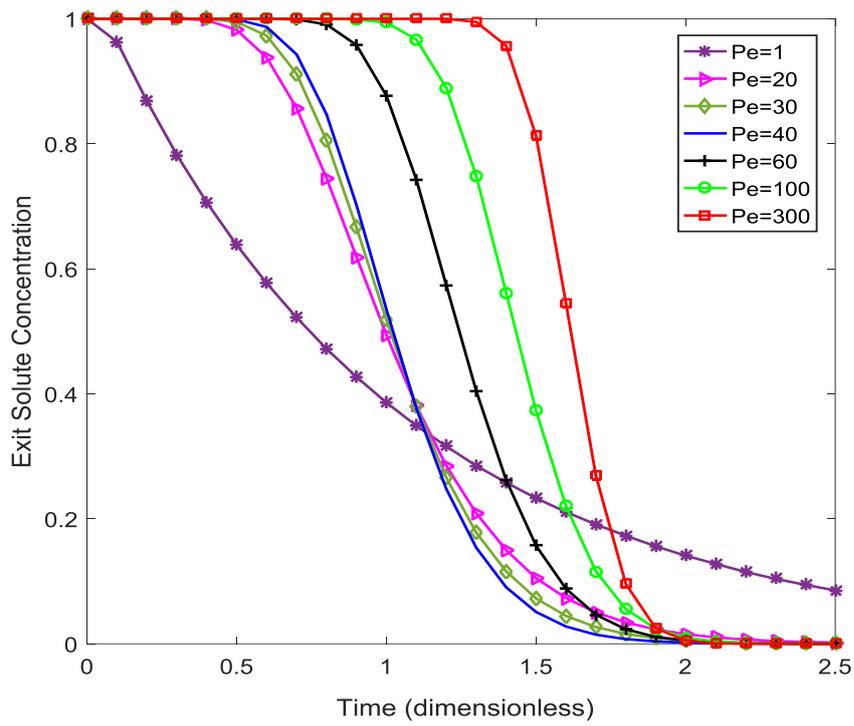
Figure 6.38 Comparison of exit solute concentration profile for different values of *Pe*.
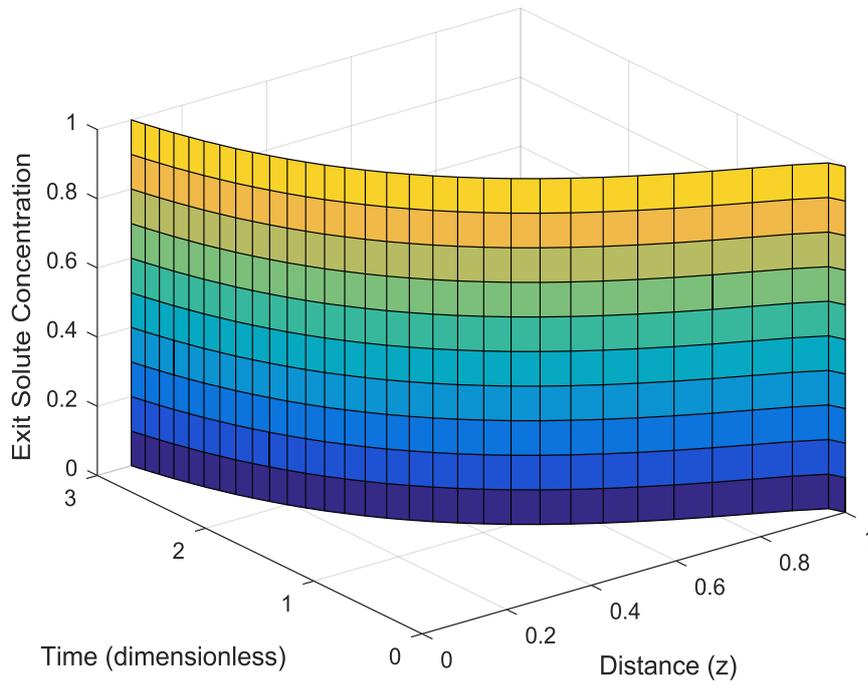
Figure 6.39 3D plot for concentration profile at exit level for *Pe*=1
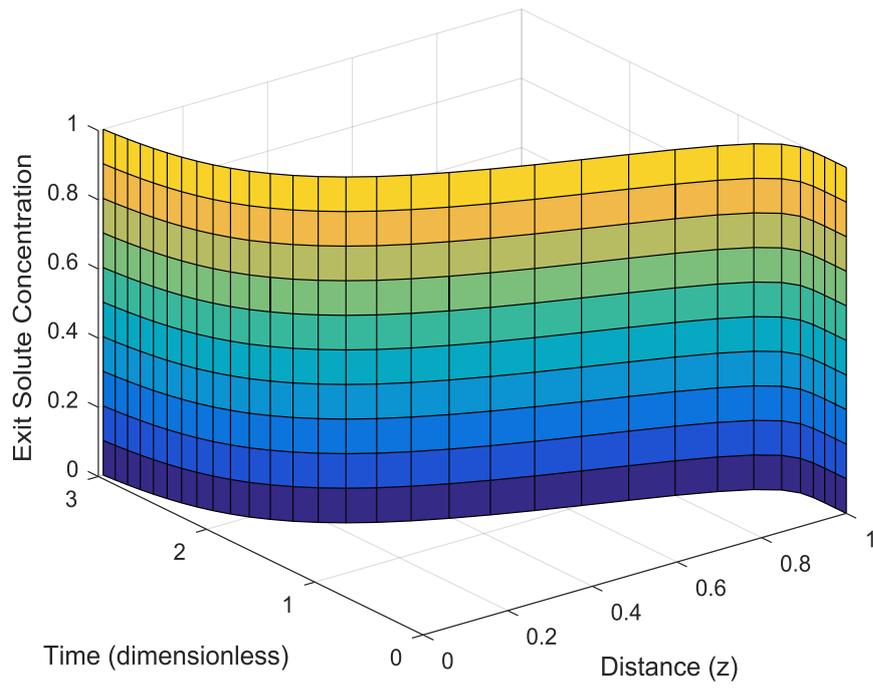
Figure 6.40 3D plot for concentration profile at exit level for *Pe*=10
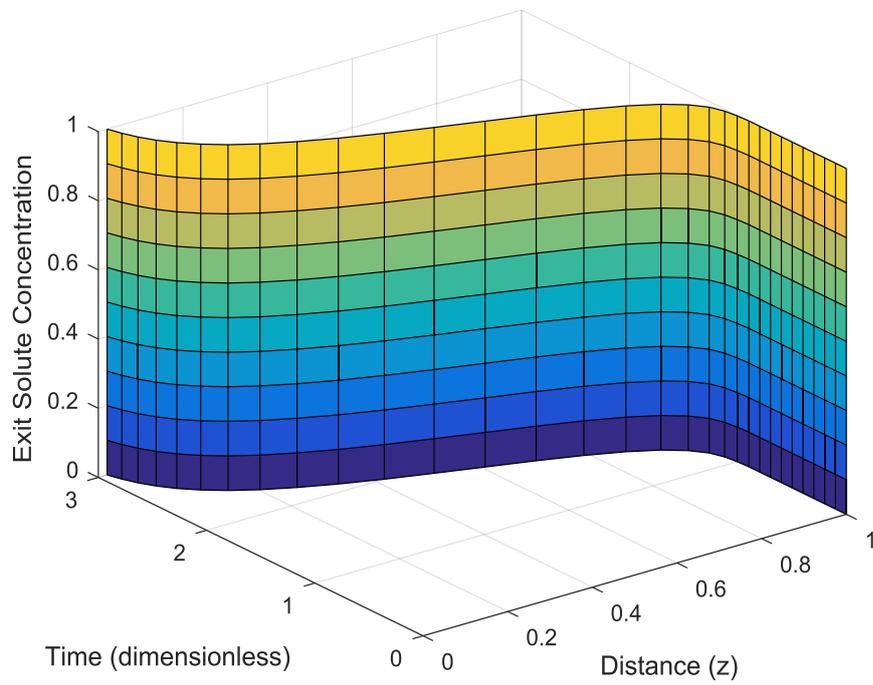
Figure 6.41 3D plot for concentration profile at exit level for *Pe*=40
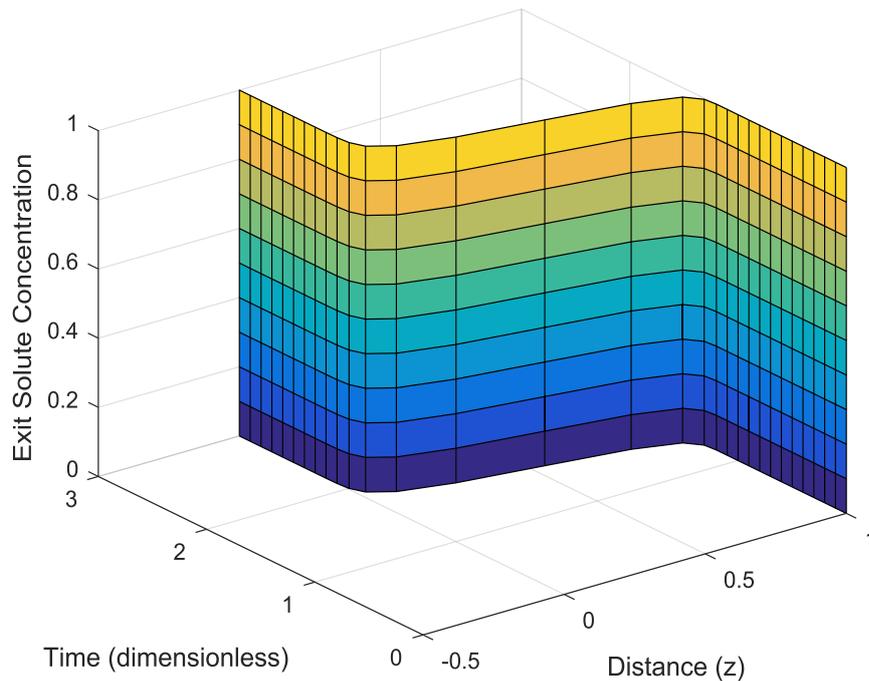
Figure 6.42 3D plot for concentration profile at exit level for *Pe*=300

In Figure 6.38, the solution profiles for exit solute concentration for different range of *Pe* lying from 1 to 300 is shown. The concentration profiles at the exit level are overlapping with each other for *Pe*=20,30 and40. In the case when *Pe* is increased from 100, the exit solute concentration is more peaked with more rate of convergence. On the other hand, when *Pe* is small, the exit solute concentration profile is more curved with a very slow rate of convergence. It is also noticed that when *Pe* is large, the concentration profile behavior is more or less the same. Also, the concentration profile at exit solute is very steep for a very small value of *Pe* which indicates that the solute takes a long period to diffuse out from the pores of the particle. However, when the value of *Pe* lies in the medium range, a long time is required for washing which results in the convergence of concentration profiles slow but is considered still as a range of acceptability.

It is also noticed that when the value of *Pe* increases, the washing time decreases. This is a situation in which each differential component of the introduced solvent immediately blends with substances of the bed and the same quantity of fluid is supplanted from the bed. This makes the bed behave like a complete mixing chamber. When the value of *Pe* is small, the diffusion performs its leading role because the value of interstitial velocity is very small. As a result, slow convergence of the concentration

profiles at exit solute is seen in Figure 6.38. This kind of state is generally not considered ideal in industrial practice. It points toward the fact that D_L becomes smaller for the high value of Pe. This affects the concentration of solute at the exit level as solute diffuses out in large amounts from the pores of the particle. In this situation, the equation is reduced into a PDE of order one. The interstitial velocity plays a major role in comparison to D_L. The concentration profile at the exit level becomes wider and washing time drops very speedily as shown in Figure 6.38. This is a state where the original contents (black liquor) of the pulp bed are forced out by the displacing fluid in a piston-like manner. But this is not a practical state because neither the interstitial velocity be infinite, nor the diffusion is zero. In an ideal situation, all the soluble impurities can indeed be removed from the pulp bed. Hence, the best possible range of Pe is needed in the industries to maintain the equilibrium between the elimination of contaminations and the washing time. Al-Jabari et al. (1994) proved that the best stage of washing can be attained for $Pe=40$. The real flow lies within the in-between range of the case of perfect mixing ($Pe=0$) and the case of perfect displacement ($Pe=\infty$) when the cake thickness and interstitial velocity are constant. For high values of Pe, the mass transfer zone is noticed as steeper. Also, the figure shows that in the case of small Pe, the solute takes more time to diffuse out from the pores of the particle. The numerical results for $Pe=1,10,40$ and 300 are also represented by 3D plots from Figures 6.39 to 6.42. Ganaie et al. (2014) explained, and the process of solute removal is simulated more perfectly with the nonlinear isotherm as compared to the linear one. Ganaie et al. (2014) considered the nonlinear model with boundary conditions same as Singh et al. (2008) and Mittal et al. (2013).

6.9 VERIFICATION OF THE TWO-DIMENSIONAL MODEL

The model is solved using the technique of QHCM and the numerical results for the solution profile are presented for distinct values of parameters. The validity is checked by applying the present technique to the above model equations for experimental data of Arora and Potůček (2012). The comparisons with previously published results in the radial and axial domain are also offered in this work.

6.9.1 Comparison Between Experimental and Numerical Values

The numerical values for solution profiles using the present technique are determined and compared with experimental values given in detail by Arora and Potůček (2012). The numerical results derived using the present method for Pe=20.81, Biot number (Bi)=10, and bed porosity(e)=0.6711 are compared with the previously published results of Arora and Potůček (2012) using OCFE and of Gupta et al. (2015) using CSCM. The comparisons are also made in terms of absolute and relative errors. Notably, the relative error in Table 6.21 is found to be very less using QHCM in comparison to OCFE and CSCM. It indicates the validity of the given model. This substantiates that QHCM is superior to these techniques. Besides this, the results obtained using the present method for $Pe = 4.91$, $\varepsilon = 0.61$, and $Bi = 4.5$ are compared in the form of absolute error with the numerical results derived with OCFE by Arora et al. (2020) and presented in Figure 6.43. The figure displays that the results using QHCM are with less absolute error than the technique OCFE.

Table 6.21. Comparison between experimental and numerical values with published results

Experimental results Arora and Potůček (2012)	Numerical results (OCFE) Arora et al. (2020)	Relative error with OCFE	Numerical results (CSCM) Gupta et al. (2015)	Relative error with CSCM	Present method QHCM	Relative error with QHCM
1.0000E+00	1.0000E+00	0.0000E+00	-	-	1.0000E+00	0.0000E+00
9.9000E-01	9.9972E-01	9.8182E-03	9.9070E-01	7.0707E-04	9.9010E-01	1.0101E-04
9.3850E-01	9.3953E-01	1.0975E-03	9.3790E-01	6.3932E-04	9.3800E-01	5.3277E-04
8.1690E-01	8.1652E-01	4.6517E-04	8.1580E-01	1.3466E-03	8.1710E-01	2.4483E-04
6.7430E-01	6.7366E-01	9.4913E-04	6.7360E-01	1.0381E-03	6.7500E-01	1.0381E-03
5.3350E-01	5.3573E-01	4.1799E-03	5.3430E-01	1.4995E-03	5.3380E-01	5.6232E-04
4.5600E-01	4.5244E-01	7.8070E-03	4.5710E-01	2.4123E-03	4.5530E-01	1.5351E-03
3.5560E-01	3.5773E-01	5.9899E-03	3.5460E-01	2.8121E-03	3.5610E-01	1.4061E-03
2.6850E-01	2.6648E-01	7.5233E-03	2.6740E-01	4.0968E-03	2.6910E-01	2.2346E-03
1.8490E-01	1.8592E-01	5.5165E-03	1.8910E-01	2.2715E-02	1.8530E-01	2.1633E-03
1.0950E-01	1.0866E-01	7.6712E-03	1.0560E-01	3.5616E-02	1.0900E-01	4.5662E-03
4.2940E-02	4.2893E-02	1.0946E-03	-	-	4.2980E-02	9.3153E-04
5.4230E-03	5.4413E-03	3.3745E-03	-	-	5.4300E-03	1.2908E-03
1.8750E-03	1.8612E-03	7.3600E-03	-	-	1.8680E-03	3.7333E-03
9.5800E-04	9.6388E-04	6.1378E-03	-	-	9.6400E-04	6.2630E-03
5.8500E-04	5.8501E-04	1.7094E-05	-	-	5.8400E-04	1.7094E-03
5.0700E-04	5.0883E-04	3.6095E-03	-	-	5.0600E-04	1.9724E-03
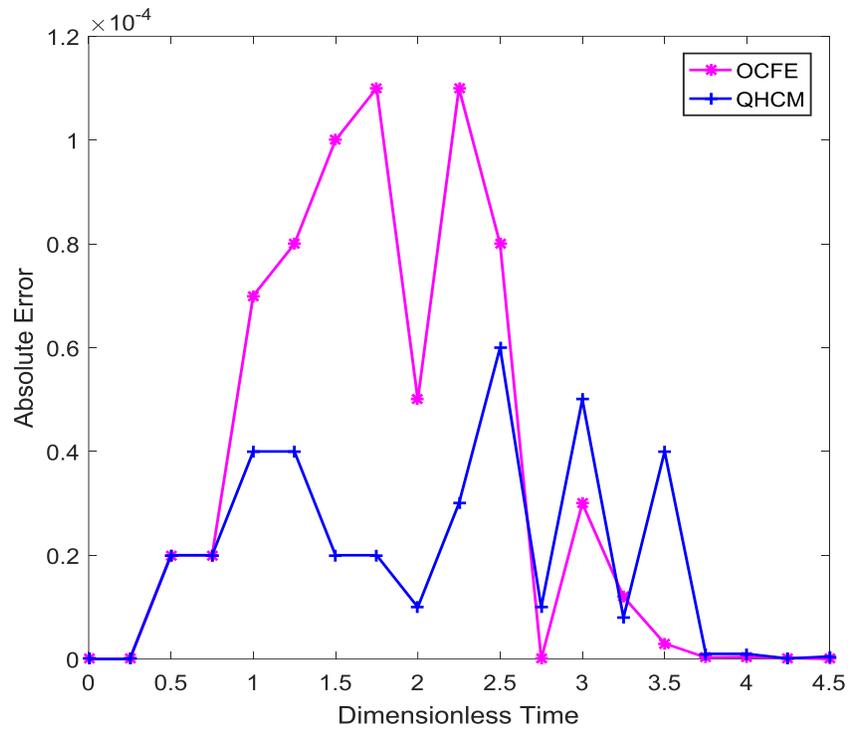
Figure 6.43 Comparison of OCFE and QHCM in terms of absolute error

6.9.2 Effect of Some Important Parameters

Practically, it is not possible that the washing process depends on a single parameter. It depends on various parameters such as a change in bed porosity, pore radius, permeability, D_L, u, Bi, and Pe. The effect of some of the essential parameters using values of experimental data of Arora and Potůček (2012) is shown graphically in this part.

Influence of Pe

The Pe is inversely proportional to dispersion, and it is lower when the dispersion is higher. Gupta et al. (2015) also proved that the dispersion coefficient has a significant effect on concentration profiles. When the value of *Pe* is increased, the dispersion coefficient decreases, and it causes a reduction in back mixing. Due to this, the adsorbed impurities of particle surface are leached in a better manner and improved washing is attained. The results in Figure 6.44 are demonstrated for the range of *Pe* from 2 to 20, *Bi*=10 and bed porosity as 0.6711. It is observed that the concentration decreases with an increase in time. The figure also declares that the tail of concentration profiles

gets longer for a small value of *Pe* as compared to a large value of *Pe* which causes an increase in back-mixing and time for washing.

Influence of the distribution ratio

The distribution ratio (D_f/R^2) plays a vital role in concentration profiles and the effect is represented in Figure 6.45. The influence of distribution ratio on solution profiles at exit level is shown for parameter *Pe*= 20.81, *Bi* = 10 and $\varepsilon = 0.67$. An increase in the value of ψ accompanied by the decrease in the value of D_f, causes the solution profiles to converge to zero more rapidly. It is shown in the figure that with the increase in the value of distribution ratio, ψ decreases which results in the increase in the retention time. Due to this fact concentration profiles are elongated and take large time to converge to the steady state condition. A small distribution ratio causes more bulging in pores and more diffusion is caused due to particle pores which results in improved washing.

Influence of Biot number (Bi)

Besides the Pe, there also exist other parameters that affect the whole process. The solution profile using QHCM is obtained for experimental conditions of washing runs by Arora and Potůček (2012) given in Table 6.22. The numerical results are presented as breakthrough curves in Figure 6.46. It is seen from this figure that the concentration of solute presented as solution profiles for washing run IV and *Pe* = 12.96 needs more time for converging to a steady-state condition in comparison with other experimental values for *Pe* = 12.25,16.92 and *Pe* = 20.8. The figure shows that the behavior of solution profiles for washing runs 1 and II are nearly similar but the *Pe* = 12.25 and *Pe* = 20.81 are not the same.

The reason is *Bi* which is also a significant parameter used to represent the mass transfer resistances on and inside the particle surface in the washing process. For washing run II the *Bi* is more than the run1 and this causes an increase in the deletion rate of adsorbed impurities on the surface of the particle. Also, it is noticed that large values of *Bi* cause an increase in mass transfer rate and indicate the fast convergence of solution profiles as compared to small *Bi*.
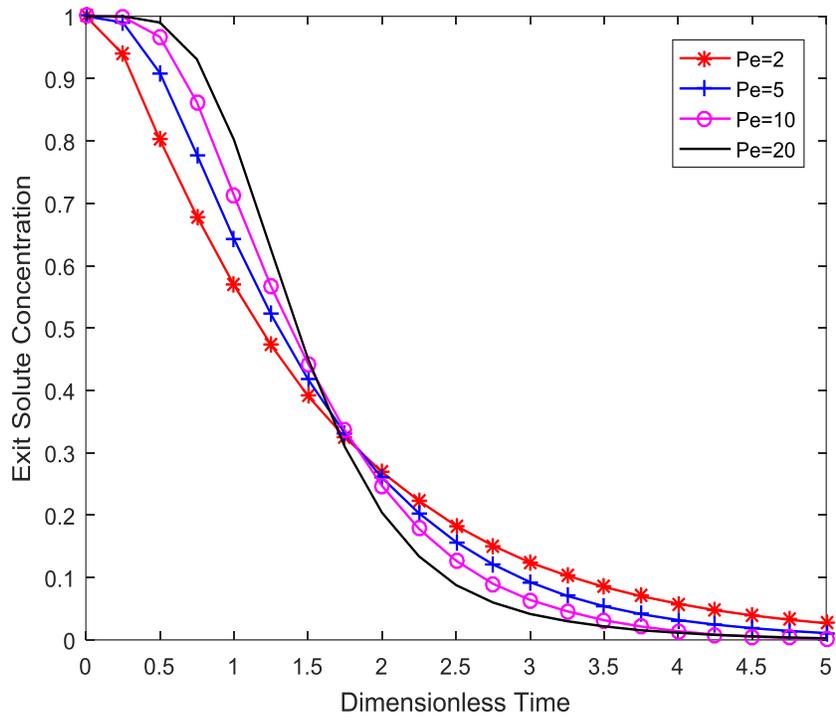
Figure 6.44 Influence of Pe on the concentration of solute at exit level
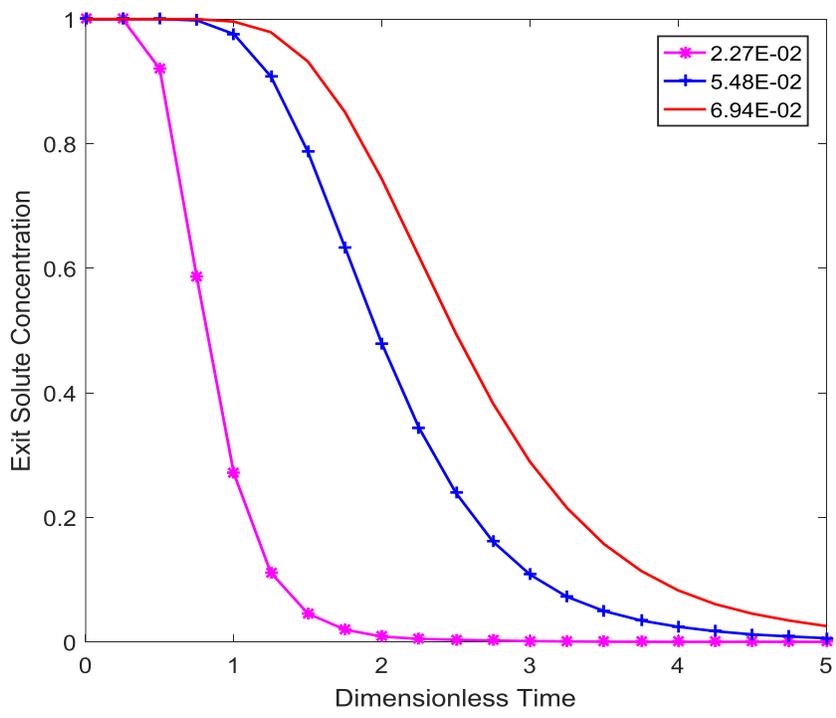
Figure 6.45 Influence of distribution ratio (D_f/R^2) on the concentration of solute at exit level
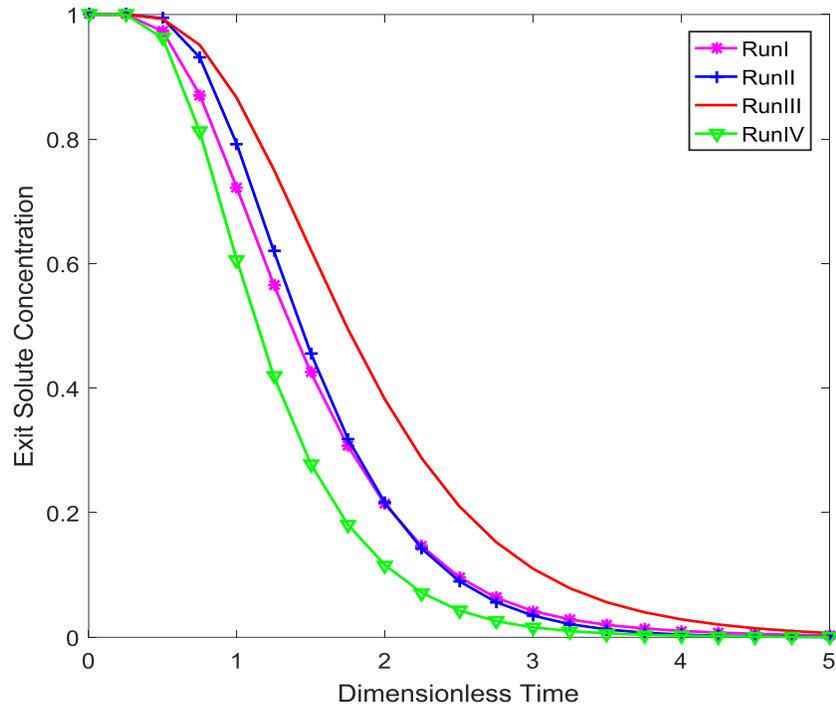
Figure 6.46 Effect of different washing run of Table 6.22 on solution profiles

Table 6.22 Experimental data for different washing runs by Arora and Potůček (2012)

Washing runs	Peclet number (*Pe*)	Biot number (*Bi*)	Fibre consistency (*C$_F$*)	Bed porosity (*e*)
Run I	12.25	7.4	12.09	0.6898
Run II	20.81	10	11.91	0.6711
Run III	16.92	7.5	13.14	0.5561
Run IV	12.96	6.3	7.96	0.8120

Influence of bed porosity(e)

Although from Figure 6.46, the *Pe* and *Bi* are nearly the same in washing runs I and IV but concentration profiles at exit level are not the same. This happens due to bed porosity which is lesser in the former case in comparison to the latter ones. The solution profile needs extra time to converge for the steady-state condition. Bed porosity (*e*) indicates the proportion of volume present for flow wash liquid to the total capacity. Also, the greater bed porosity shows the availability of

more volume for displacement, and hence the absorbed impurities on the particle surface are leached away in a better manner.

Influence of mass transfer coefficient (k)

The effect of mass transfer coefficient (k) on the breakthrough curves is shown in Figure 6.47. For higher values of k, the detachment rate becomes small and accordingly more time is consumed by the solution profiles to converge to steady state condition. It is observed from figure that effective washing is achieved for smaller values of mass transfer coefficient.
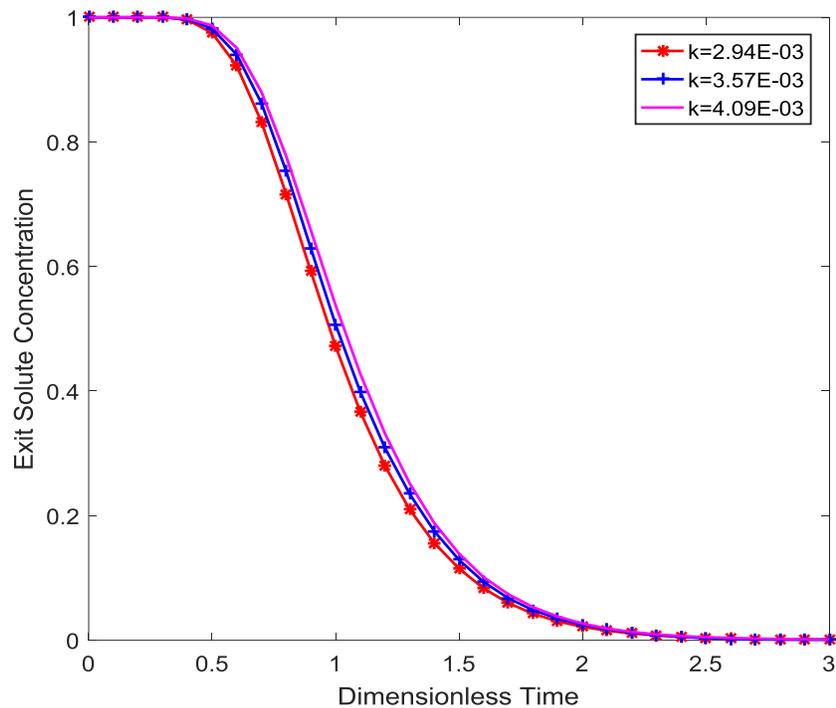
Figure 6.47 Effect of mass transfer rate (k) on solution profiles

6.10 SUMMARY

In this chapter, the linear models discussed earlier are solved with QHCM and numerical results are compared with the analytic solution as well as with previous numerical techniques using error analysis. Besides this, the stability and convergence of the method are also examined. Thereafter, the nonlinear models are solved, and numerical results obtained are found to be better than earlier techniques. The numerical results are also simulated with industrial data of different paper mills available in the literature. At last, the two-dimensional model is solved with this technique, and important parameters affecting the process are also explained.

Contents of this chapter are published in:

1. *Afrika Matematika, Vol. 32(5) 997-1019, 2021, ISSN: 2190-7668. (Scopus indexed).*
2. *Journal of Engineering Research, Vol. 10 (1A), 67-77, 2021, ISSN: 2307-1885 (SCIE).*
3. *Advances and Applications in Mathematical Sciences, 20(11) 2549-2557, 2021, ISSN: 0974-6803 (UGC-Care).*
4. *Advances in Intelligent Systems and Computing, Vol. 1412, 995-1009, 2022 Springer Nature, ISSN: 2194-5357(Scopus indexed).*